1.0

1.1

1.25   1.4   1.6

2.8   2.5
3.2   2.2
3.6
4.0   2.0

1.8

MICROCOPY RESOLUTION TEST CHART
NATIONAL BUREAU OF STANDARDS-1963-A

DAVID W. TAYLOR NAVAL SHIP
RESEARCH AND DEVELOPMENT CENTER

Bethesda, Md. 20084

WAVE EXCITATION AND VERTICAL PLANE

OSCILLATION EXPERIMENTS ON A HIGH

LENGTH-TO-BEAM RATIO SURFACE EFFECT SHIP

by

James A. /Fein

and

Lawrence O. /Murray

APPROVED FOR PUBLIC RELEASE: DISTRIBUTION UNLIMITED

SHIP PERFORMANCE DEPARTMENT

77 p.

July 1976

SPD-697-01

1473

389694

LB

MAJOR DTNSRDC ORGANIZATIONAL COMPONENTS

```
                          ┌──────────────────────┐
                          │       DTNSRDC        │
                          │     COMMANDER        │
                          │                  00  │
                          │  TECHNICAL DIRECTOR  │
                          │                  01  │
                          └──────────┬───────────┘
                                     │
        ┌──────────────────────┐     │     ┌──────────────────────┐
        │  OFFICER-IN-CHARGE    │─────┴─────│  OFFICER-IN-CHARGE    │
        │    CARDEROCK          │           │    ANNAPOLIS          │
        │                  05   │           │                  04   │
        └──────────────────────┘           └──────────────────────┘

        ┌──────────────────────┐
        │    SYSTEMS            │
        │   DEVELOPMENT         │─────────────┐
        │   DEPARTMENT      11  │             │
        └──────────────────────┘             │

        ┌──────────────────────┐     ┌──────────────────────┐
        │  SHIP PERFORMANCE    │     │   AVIATION AND       │
        │   DEPARTMENT         │─────│  SURFACE EFFECTS     │
        │                  15  │     │   DEPARTMENT     16  │
        └──────────────────────┘     └──────────────────────┘

        ┌──────────────────────┐     ┌──────────────────────┐
        │   STRUCTURES         │     │  COMPUTATION,        │
        │   DEPARTMENT         │─────│  MATHEMATICS AND     │
        │                  17  │     │  LOGISTICS DEPARTMENT│
        └──────────────────────┘     │                  18  │
                                     └──────────────────────┘

        ┌──────────────────────┐     ┌──────────────────────┐
        │  SHIP ACOUSTICS      │     │  PROPULSION AND      │
        │   DEPARTMENT         │─────│  AUXILIARY SYSTEMS   │
        │                  19  │     │   DEPARTMENT     27  │
        └──────────────────────┘     └──────────────────────┘

        ┌──────────────────────┐     ┌──────────────────────┐
        │   MATERIALS          │     │   CENTRAL            │
        │   DEPARTMENT         │─────│  INSTRUMENTATION     │
        │                  28  │     │   DEPARTMENT     29  │
        └──────────────────────┘     └──────────────────────┘
```
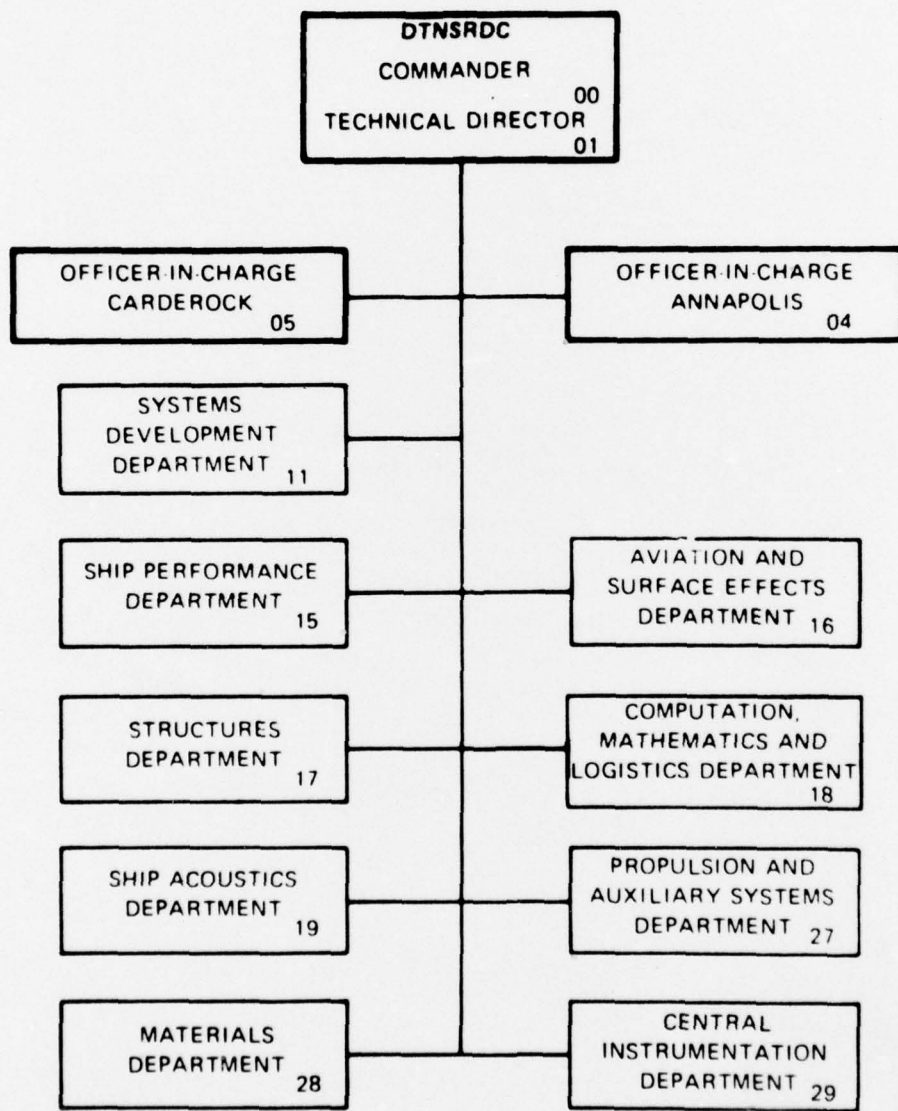
REPORT DOCUMENTATION PAGE		READ INSTRUCTIONS BEFORE COMPLETING FORM
1. REPORT NUMBER SPD-697-01	2. GOVT ACCESSION NO.	3. RECIPIENT'S CATALOG NUMBER
4. TITLE *(and Subtitle)* Wave Excitation and Vertical Plane Oscillation Experiments on a High Length-To-Beam Ratio Surface Effect Ship		5. TYPE OF REPORT & PERIOD COVERED
		6. PERFORMING ORG. REPORT NUMBER
7. AUTHOR(s) J. A. Fein and L. Murray		8. CONTRACT OR GRANT NUMBER(s)
9. PERFORMING ORGANIZATION NAME AND ADDRESS David W. Taylor Naval Ship R&D Center Bethesda, Maryland 20084		10. PROGRAM ELEMENT, PROJECT, TASK AREA & WORK UNIT NUMBERS GHR Work Unit Number 1572-128
11. CONTROLLING OFFICE NAME AND ADDRESS		12. REPORT DATE July 1976
		13. NUMBER OF PAGES 68 pages
14. MONITORING AGENCY NAME & ADDRESS(if different from Controlling Office)		15. SECURITY CLASS. (of this report) UNCLASSIFIED
		15a. DECLASSIFICATION/DOWNGRADING SCHEDULE

16. DISTRIBUTION STATEMENT (of this Report)

APPROVED FOR PUBLIC RELEASE: DISTRIBUTION UNLIMITED

17. DISTRIBUTION STATEMENT (of the abstract entered in Block 20, if different from Report)

18. SUPPLEMENTARY NOTES

19. KEY WORDS (Continue on reverse side if necessary and identify by block number)

20. ABSTRACT (Continue on reverse side if necessary and identify by block number)

Captive model experiments were conducted on a high length-to-beam ratio surface effect ship testcraft design to determine vertical plane characteristics and to evaluate captive model experimental techniques. Model results for forced heave oscillation and pitch oscillations, and regular-wave exciting forces and moments and transient-waves exciting forces and moments are reported. The effects of sidewalls and cushion pressure variation on the oscillation results are identified. The correlation between the regular waves and transient waves techniques for determining ~~the excitation is shown~~

DD FORM 1473
1 JAN 73   EDITION OF 1 NOV 65 IS OBSOLETE
S/N 0102-014-6601

UNCLASSIFIED

TABLE OF CONTENTS

LIST OF FIGURES

LIST OF FIGURES (Cont'd)

Page

v

LIST OF FIGURES (Cont'd)

NOMENCLATURE

$\bar{F}$	vertical wave exciting force
g	gravitational constant
$\dot{h}$	velocity in the h - direction, time derivative of h
$\ddot{h}$	acceleration in the h - direction, time derivative of $\dot{h}$
h_o	amplitude of heave oscillation in feet
h_w	wave height
I_y	pitch moment of inertia (about y-axis)
l	length of cushion, characteristic length
m	design mass
M	moment about y-axis (pitching moment)
$\bar{M}$	wave exciting moment in pitch
M_1	pitching moment in-phase with the oscillation measured by the block gages
M_2	pitching moment out-of-phase with the oscillation measured by the block gages
M_h	partial derivative of M with respect to h, pitching moment-static heave coupling derivative
$M_{\dot{q}} = M_{\dot{\theta}}$	partial derivative of M with respect to q, pitch damping derivative
$M_{\dot{q}} = M_{\dot{\theta}}$	partial derivative of M with respect to $\dot{q}$, pitch added moment of inertia derivative
M_w	partial derivative of M with respect to w, pitch moment-heave velocity coupling derivative
$M_{\dot{w}}$	partial derivative of M with respect to $\dot{w}$, pitch moment-heave acceleration coupling derivative
M_θ	partial derivative of M with respect to θ, pitch restoring moment derivative

vii

q	rotational velocity about y-axis, pitch rate
$\dot{q}$	rotational acceleration about y-axis, pitch acceleration
t	time
U	resultant veloctiy
w	velocity in the z-direction
$\dot{w}$	acceleration in the z-direction
$\bar{x}$	distance between struts of planar-motion-mechanism
x,y,z	body-fixed right-handed coordinate system with directions indicated in Figure 1
x',y',h	inertial right handed coordinate system, fixed with respect to the water system
Z	force in the z-direction (also referred to as heave force)
Z_1	heave-force in-phase with the oscillation
Z_2	heave force out-of-phase with the oscillation
Z_h	partial derivative of Z with respect to h, static restoring derivative
$Z_q = Z_{\dot{\theta}}$	partial derivative of Z with respect to q, static force-pitch rate coupling derivative
$Z_{\dot{q}} = Z_{\ddot{\theta}}$	partial derivative of Z with respect to $\dot{q}$, heave force-pitch acceleration coupling derivative
Z_w	partial derivative of Z with respect to w heave damping derivative
$Z_{\dot{w}}$	partial derivative of Z with respect to $\dot{w}$, heave added mass derivative
Z_θ	partial derivative of Z with respect to θ, heave force-static pitch angle coupling derivative
$\hat{Z}, \hat{M}$	amplitudes of the total vertical force and pitching moment

α	angle of attack
δ	pitch exciting moment phase angle with respect to the wave at the CG
θ	pitch angle, positive bow up, (equal to sine for small angles)
$\dot{\theta}$	pitch rate (same as q)
$\ddot{\theta}$	pitch acceleration (same as $\dot{q}$)
θ_0	amplitude of pitch oscillation (equal to α/X for small angles)
ϵ	heave exciting force phase angle with respect to the wave at the CG
ρ	density of water (1.936 slugs/ft^3)
ΣM	sum of the pitching moments measured by the gages
ΣZ	sum of the forces in the z-direction measured by the gages
ϕ	phase angle between the oscillation and the resultant force vector
ϕ_s	phase angle between the struts of a planar-motion-mechanism
ω	frequency of oscillation in radians/sec
ω_e	encounter frequency

<u>Nondimensional Quantities</u> (defined in text equation (17))

H	nondimensional heave exciting force
M_ψ	nondimensional pitch exciting moment
μ_e	nondimensional encounter frequency

ABSTRACT

Captive model experiments were conducted on a high length-to-beam surface effect ship testcraft design to determine vertical plane characteristics and to evaluate captive model experimental techniques. Model results for forced heave oscillation and pitch oscillations, and regular-wave exciting forces and moments and transient-waves exciting forces and moments are reported. The effects of sidewalls and cushion pressure variation on the oscillation results are identified. The correlation between the regular-wave and transient-waves techniques for determining the excitation is shown.

INTRODUCTION

The initial objective of this experimental investigation was to compare the results of two oscillation techniques which could be applied to surface ship models: the body-fixed coordinate system approach which requires a planar-motion mechanism (PMM) and is utilized by stability and control investigators, and the free surface-fixed inertial coordinate system technique employed by seakeeping investigators using a single strut pitch-heave oscillator or PMM.

These two oscillator techniques should provide derivatives that are equivalent when a coordinate transformation is imposed. Establishing this equivalence would allow one experiment to provide information for both applications if the frequency range was appropriately chosen. Although the results from body-fixed axis defined pitching were inconsistent in this case, it is shown that the seakeeping pitch-heave oscillator approach can provide all the pertinent information for stability investigations.

A surface effect ship (SES) model, in particular, the high length-to-beam ratio SES model (designated as XR-5) was chosen because no information on vertical plane coefficients was available on any SES.

In retrospect, the use of an SES model may have added to the complexity of the experiment, making conclusive results about the oscillation techniques more elusive. However, the opportunity to test the XR-5 in a captive condition provided data in two related areas that are reported herein. One was the determination of the sidewall contribution to the overall stability derivatives and the other was the acquisition of

2

wave excitation forces and moments in head seas by both regular wave and transient-waves techniques. This last effort permitted the development of a computer simulation of craft motions in head seas that could be compared to free model results. The transient waves technique was applied to wave excitation force determination (for the first time to the authors' knowledge) and produced results that agreed very well with the regular wave results.

This report contains a description of the model, a discussion of the various experiment techniques and apparatus, a treatment of the data analysis techniques including the coordinate system effects, a presentation of the results and pertinent recommendations and conclusions.

DESCRIPTION OF MODEL

The model was a one-third scale version of a 40-foot manned XR-5 testcraft. The XR-5 was designed at the David W. Taylor Naval Ship Research and Development Center (DTNSRDC) and has been involved in trials at Patuxent Naval Air Station to prove the feasibility of the concept and perhaps lead to larger size designs. The full scale craft size and mission was not of importance for the experiment described herein, since its purpose was to evaluate experimental techniques for SES craft in general.

The model configuration is shown in Figure 1 and model characteristics are given in Table 1. The model was constructed of polyurethane foam reinforced with a coating of fiberglass. The bow and stern seals were semi-rigid, three-lobed and of the semi-planing type and were inflated directly from stacked axial flow fans. The cushion was fed

3

through ducts from the seals, shown in Figure 1, and directly from up to eight fans located in the main plenum. The fan configuration was designated by the number of fans operating in the bow, main section, and the stern respectively; i.e. 2-3-2 meant two fans in each seal with three plenum fans operating. Fans not in use had cover plates to prevent loss of air through them. Fans could operate at only one speed, 20,000 rpm. Duct settings were chosen to correspond to those used in Reference 1, so that the model configuration would be the same as that used in the most recent motions experiments.

Each seal height was regulated by two sets of cables that maintained a maximum downstop position. The downstop position could be modified by using shims to adjust the length of the cables.

The model sidewalls had a 45 degree deadrise angle. The model was not powered or capable of self propulsion, though the manned test-craft had two outboard motors for powering.

DESCRIPTION OF EXPERIMENTAL APPARATUS

This experiment was designed so that both the captive model oscillation runs and the captive model wave excitation runs could be made without changing the model towing apparatus. The facility chosen was the Center's Deep Water Basin (Carriage II). This tank permitted the required speed of 12 knots and has the depth and width necessary to avoid interference effects. In addition, the wavemaker in this tank was suitable for producing good regular and transient waves at those frequenies and amplitudes of interest.

The tow rig and oscillator selected was the DTNSRDC Planar-Motion-Mechanism Mark I; a two strut sinusoidal oscillator with a fixed amplitude and three fixed frequencies, but variable phase between the struts. This device was chosen because it allowed for the examination of the pitching motion in both the body axes and fixed axes systems with the same set-up, though only at three discrete frequencies. The amplitude was chosen to assure that linearity was preserved in the oscillation experiments. A complete description of the oscillator is given in Reference 2.

The block gage arrangement shown in Figure 1 allowed for the struts to be placed equidistant from the design longitudinal CG. The model was ballasted to this CG location thus eliminating some inertial terms in the analysis equations. The weight of the instrumented model exceeded the design weight, but this effect could be removed from the data.

Each gage assembly consisted of two four-inch block gages: one oriented to measure the axial force and the other oriented to measure the vertical force. The pitch pivots were located at the base of the struts which enabled a pitch moment to be measured based on the difference between the two vertical force readings and referenced about a point half way between the struts.

The planar-motion-mechanism was mounted on the vertical rails on the east end of Carriage II with the model heading west; i.e. toward the wavemaker.

In addition to the block gages, the model instrumentation included a potentiometer located on each strut, and two pressure transducers of the Endevco type; one to measure the bow seal pressure, the other to

5

monitor cushion pressure amidships. Wave height was measured by an ultrasonic probe located well in front of the model.

EXPERIMENTAL PROCEDURES

The experiments consisted of heaving oscillations, inertially defined pitch oscillations, body axes defined pitch oscillations, regular-wave excitations and transient-wave excitation. In addition. the model was towed at various heave heights and trim angles to obtain the static and restoring coefficients and to determine the proper flying height for the dynamic experiments.

Statics

The model was set to the specified trim by deflecting the tilt table, and the block gages were zeroed with the model fully out of the water. The model was then lowered down the vertical rails to the specified height and the fans were actuated. With fans running and the carriage standing still, a data reading was taken. The carriage was then started and another data record was taken at the proper speed. The heave position for each speed for the remaining experiments was determined by finding the point where the cushion and sidewalls were generating a vertical force equal to the design weight. The trim conditions were based on the values from free-to-trim model experiments.

Oscillations

The oscillations, (essentially sinusoidal perturbations in heave and in pitch) were conducted about the equilibrium conditions. For heave, the two oscillation techniques were equivalent in that both struts moved in

unison. The heaving oscillation was conducted at all three set frequencies for the test conditions. The model was oscillated in air and on the surface at three forward speeds. The 2-0-2 fan configuration was evaluated at all speeds while the 2-3-2 fan configuration was evaluated only at 12 knots.

At 9 knots, the model was oscillated in heave about the mean heave level with the fans off and seals taped up so that sidewall effects could be identified.

The pitching oscillation, defined with respect to axes fixed in the water surface and referred to as inertial pitching, consisted of a 180 degree phase lag of the stern strut with respect to the bow strut so that the bow and stern vertical movements always opposed each other. This motion was not dependent on model speed as the coordinate system was unaffected by the motion, which was not the case for the body fixed axes system. Inertial pitching oscillations were conducted for all the conditions where heaving oscillations were also conducted.

The body-fixed axes pitching motion required that the model angle of attack, as defined in body axes, equal zero; i.e. that the model's longitudinal axis always be tangent to the path of the CG. This condition was met when there was a phase angle ϕ_S between the struts derived from the expression;

$$\tan\frac{\phi_S}{2} = \frac{\omega\bar{x}}{2U} \quad \text{where } \bar{x} \text{ is the strut spacing} \quad (1)$$

When U=0 this reduced to ϕ_S = 180 degrees, which agreed with the inertial pitching motion.

The body axes pitching motion definition had been utilized in the submarine area and as body-axes yawing for horizontal plane motions (maneuvering) of ships where the equations of motion were written in body-fixed axes.

7

The water-fixed axes definition had been utilized for vertical plane

behavior (seakeeping) of surface ships where an inertial frame is assumed.

As shown in the section on analysis of results, the pitching forces and

moments in either coordinate system could be reported in terms of the

other with an appropriate correction that depended on the heaving and

statics results. The objective of this effort was to see whether the

two oscillation techniques actually produced the same numerical values

when appropriate corrections were made.

Wave Excitations

For the wave excitation experiments, the model was held captive at its

equilibrium attitude while towed through waves, and the resultant forces

and moments were measured. These results would be applicable to head

seakeeping analyses on the assumption that a linear response of the model

was achieved within the range of experimental results. This assumption

may not be valid for all designs.

The regular waves were generated with periods ranging from 1.25

seconds to 3.4 seconds and an approximate double amplitude of 3 inches

(0.076 meters). The frequency range was chosen to give a realistic selec-

tion of wave lengths within the limits of the wavemaker. The double am-

plitude of 3 inches gave a measurable signal without violating linearity.

The transient wave technique was first developed in Reference 3

where it was applied to the motions of conventional displacement ships.

The transient wave packet contained energy at all the pertinent frequen-

cies so that a full range of motion response resulted when the non-captive

8

model passed through the wave during a single pass down the basin. The transient technique was proposed to replace regular wave experiments for the determination of motions and good correlation was shown. In a like manner the sinusoidal, linearly varying transient wave developed in Reference 3 and Reference 4 was applied in the wave excitation force and moment problem. The reasoning in favor of its use in the present case was the reduction of time involved in testing since one transient wave run could replace up to twenty regular wave experiments.

The use of a captive model avoided some problems encountered in free model transient wave work. The electrical transducers of the block gages are excited at 400 cycles per second and thus respond to the changing wave frequencies much faster than a free model where bearing friction can limit response at high frequencies. This allowed testing at Froude numbers close to 1.0 where the encounter frequency approached four cycles per second. It is doubtful that a free model of the XR-5 would have accurately responded to the transient waves at these high frequencies of encounter.

At the high speeds examined in this experiment, there was no indication that the model-generated wave would have affected the measured wave amplitude as had been noted in earlier investigations. The generated transient waves coalesced within 100 feet of the wavemaker in the Deep-Water Basin and consequently encountered the model after peaking. The peaks were not too pronounced and the encountered wave did not show signs of distortion. Runs had to be timed carefully to include all the waves during the pass at speed. Figure 2 shows the quality of the transient waves and the range of

9

wave frequencies included in the data run. The figure shows that the change of frequency does not affect amplitude except at two points.

The transient technique seemed well suited to the measurement of excitation forces and moments. Its use for this purpose did not violate any of the linear system assumptions made by Reference 3 in deriving the transient approach.

ANALYSIS OF DATA

The data analysis benefited greatly from the use of the Interdata computer during the test. The computer processed the data and produced the basic printouts, a sample of which is shown as Figure 3. For each run, the printout included a display of the main parameters speed and frequency of encounter. For each channel, the printout provided the mean value and an index of scatter of the data, as well as the in-phase and out-of-phase components and the amplitude and phase of each channel. In addition to showing processed results for individual force gages the printout included results for computed total forces and moments.

The pressures and strut displacements were also tabulated in this useful form. Only the transient wave results required additional after-test analysis (an on-carriage capability in this area has recently been developed as well).

Statics

The statics data consisted of the mean of the measured forces and moments. The derivatives, with respect to static pitch angle and heave displacement, were determined by testing at off-equilibrium conditions and determining the slope of the force curves about the equilbrium pitch and heave positions. Data was corrected to the proper CG location (which

10

was below the midpoint between the pitch pivots). Static runs in air demonstrated that the aerodynamic tares were negligible.

Oscillations

In considering the oscillation results, the two coordinate systems had to be considered: the body-fixed axes system (x,y,z), and the inertial (water-surface-fixed) axes system (x',y',z'). The positive directions of these coordinates are given in Figure 1.

Given that Θ is body axes pitch angle, w is body axes heave velocity, and v is constant, the systems are connected by the relations:

$$\dot{h} = w - \Theta U$$

and

$$\ddot{h} = \dot{w} - \dot{\Theta}U \tag{2}$$

for small oscillations where the "dot" denotes a time derivative.

The heaving oscillations were analyzed by converting the sinusoidal force output into components that are in-phase or 180 degrees out-of-phase with the motion. This approach is described fully in References 5 and 6.

If the 'pure' heave motion is given by:

$$h = h_0 \sin\omega t, \tag{3}$$

where h_0 is the heave amplitude, positive in the positive z-direction. Then,

$$\dot{h} = \omega h_0 \cos\omega t = w, \text{ heave velocity, and} \tag{4}$$

$$\dot{w} = -\omega^2 h_0 \sin\omega t. \tag{5}$$

11

the total heave force Z is given by:

$$\Sigma Z = \hat{Z}\sin(\omega t - \phi)$$
$$= -Z_1\sin\omega t + Z_2\cos\omega t, \tag{6}$$

where ϕ is the phase angle (lead or lag) of the force and given the definitions:

$$Z_1 = -Z\cos\phi \text{ (in-phase), and}$$
$$Z_2 = -Z\sin\phi \text{ (out-of-phase)} \tag{7}$$

There is a similar definition for pitch moment M, with magnitude $\hat{M}$:

$$\Sigma M = M\sin(\omega t - \phi)$$
$$= -(-M\cos\phi)\sin\omega t + (-M\sin\phi)\cos\omega t \tag{8}$$
$$= -M_1\sin\omega t + M_2\cos\omega t$$

The equations of motion for the heave dependent forces are given in terms of the Taylor series coefficients as follows:

$$\Sigma Z = Z_h h + Z_w w + (Z_{\dot{w}} - m)\dot{w} \text{ and}$$
$$\Sigma M = M_h h + M_w w + M_{\dot{w}}\dot{w}, \tag{9}$$

and the coefficients (also called stability derivatives) can be calculated from the equations by separating the sine and cosine terms to obtain:

$$Z_1 = -Z_h h_o + (Z_{\dot{w}} - m)\omega^2 h_o,$$
$$Z_2 = Z_w \omega h_o,$$
$$M_1 = -M_h h_o + M_{\dot{w}}\omega^2 h_o, \text{ and} \tag{10}$$
$$M_2 = M_w \omega h_o.$$

Equations (10) can be put into a useful form for each calculation by plotting the quantities Z_1, Z_2, M_1, M_2 as shown in Figure 4. This results in a simple graphical technique for interpreting oscillator results for surface models that was proposed by Magnuson in 1967 in a similar form. Figure 4 illustrates the approach but does not indicate the expected

directions of the data. The major difficulty with this approach is that frequency dependence of the dynamic derivatives is not considered. In this experiment, there was not enough data to determine frequency dependence.

In order to analyze the data obtained in the inertial pitching motion in terms of stability derivatives defined in the body fixed axes, the coupled equations of motion in pitch and heave must be considered:

$$\Sigma Z = Z_h h + Z_\Theta \Theta + Z_w w + (Z_{\dot\Theta} + mU)\dot\Theta + (Z_{\dot w} - m)\dot w + Z_{\ddot\Theta}\ddot\Theta \qquad \text{and}$$

$$\Sigma M = M_h h + M_\Theta \Theta + M_w w + M_{\dot\Theta}\dot\Theta + M_{\dot w}\dot w + (M_{\ddot\Theta} - I_y)\ddot\Theta \qquad (11)$$

In body axes terms inertial pitching implies that h=0 at the reference point, and (for Θ positive bow up)

$$\Theta = \Theta_o \sin\omega t$$

$$\dot\Theta = q = \omega\Theta_o \cos\omega t \qquad (12)$$

$$\ddot\Theta = \dot q = -\omega^2 \Theta_o \sin\omega t$$

There is an angle of attack present with respect to the body axes from equation (2) so:

$$w = \Theta U = (\Theta_o \sin\omega t)U \qquad \text{and}$$

$$\dot w = \dot\Theta U = (\omega\Theta_o \cos\omega t)U. \qquad (13)$$

Combining (11), and (12), and (13):

$$\Sigma Z = Z_\Theta(\Theta_o \sin\omega t) + Z_w(\Theta_o \sin\omega t)U + (Z_q + mU)(\omega\Theta_o \cos\omega t)$$

$$+ (Z_{\dot w} - m)(\omega\Theta_o \cos\omega t)U - Z_{\dot q}(\omega^2\Theta_o \sin\omega t) \qquad (14)$$

$$\Sigma M = M_\Theta(\Theta_o \sin\omega t) + M_w(\Theta_o \sin\omega t)U + M_q(\omega\Theta_o \cos\omega t) + M_{\dot w}(\omega\Theta_o \cos\omega t)U$$

$$- (M_{\dot q} - I_y)(\omega^2\Theta_o \sin\omega t)$$

Recalling (6) and (8) and taking the sine and cosine parts separately:

13

$$Z_1 = -(Z_\Theta + UZ_w)\Theta_0 + Z_{\dot{q}}\omega^2\Theta_0,$$

$$Z_2 = (Z_q + UZ_{\dot{w}})\omega\Theta_0,$$

$$M_1 = -(M_\Theta + UM_w)\Theta_0 + (M_{\dot{q}} - I_y)\omega^2\Theta_0 \quad \text{and}$$

$$M_2 = (M_q + M_{\dot{w}}U)\omega\Theta_0 \quad . \tag{15}$$

Equations (15) can be represented graphically as in Figure 5 which presents a simplified form, but not the likely trends in the data.

The body-axes pitching definition introduces a variable phase angle between the struts that sets w and $\dot{w}$ equal to zero. From (2):

$$\dot{h} = -\dot{\Theta}U,$$

$$\ddot{h} = -\dot{\Theta}U, \text{ and given that}$$

$$h = \dot{\Theta}U/\omega^2. \tag{16}$$

This leads to the phase angle condition on the struts given in Equation (1). Substituting into Equation (11) and following through, gives the equations for reduction of the data that are indicated graphically in Figure 6. Unfortunately, this technique did not produce results that could be compared with the inertial pitching. The results were very scattered, not repeatable, and the static intercept values did not check with those obtained from the statics. One reason for this can be seen from the equations which show that the CG moves with respect to the water surface during the body axis pitching. This heave produced large buoyancy forces that would tend to dominate the rate and acceleration effects. Thus the terms one is trying to identify are clouded by what is essentially a static tare. This leads to the scatter and error found when applying this approach to surface craft.

The inertial pitching technique was not subject to these difficulties. Contributions due to inertial heave were added to the data in Equation (15) (a relatively clean process) in order to obtain the body-

14

axis pitching terms. The magnitude of the measured terms and the correction terms could thus be monitored and compared. For these reasons the inertial pitching technique used by seakeeping investigators seemed readily adaptable to the calculation of body-axes stability derivatives. The body-axes approach used for submarines, on the other hand, seemed ill-suited to surface ship work, although more extensive investigations with other types of models should be undertaken to verify this statement.

Wave Excitation

The regular wave excitation forces and moments in the vertical plane were recorded on digital tape for analysis on the carriage by the Interdata. The data format was similar to that for the oscillation experiments and is shown on the sample data sheet in Figure 7. The wave height was measured forward of the model but corrected to the model LCG for the analysis of the phase relationships. The wave height channel was channel 2 listed as 'Reference' in Figure 7.

The quantities that were of interest were the amplitude and phase of the vertical force and pitching moment. It is important to note that the gage polarities were not changed from the oscillation test so that down directed force was still positive. Wave height was positive upward, which led to a 180 degree phase angle between heave force and wave height as frequency went to zero. Pitch moment phase angle approached 270 degrees in the zero frequency limit as expected.

The force and moment amplitude and frequency were nondimensionalized by wave height according to the standard format:

15

$$H = \frac{L \cdot \overline{F}}{h \cdot m \cdot g}$$

$$M_\psi = \frac{\overline{M}}{h \cdot m \cdot g} \quad \text{and} \tag{17}$$

$$\mu_e = \omega_e \sqrt{L/g} \quad ,$$

where $\overline{F}$ and $\overline{M}$ are the force and moment amplitudes respectively.

The transient wave data were analyzed after the experiment by the PSHAFT program transient wave option which was developed by earlier investigators. The frequency content of the measured quantities was Fourier analyzed for the full frequency range contained in the waves. The analysis process attempted to extract the maximum data from the transient wave runs, however, as the frequency was changing rapidly some scatter was evident. The quantities of interest were then nondimensionalized by the format above with the wave height for each frequency used to nondimensionalize that data point. This process tended to exaggerate the scatter in the data.

RESULTS

The statics and oscillation results are presented in Appendix A in dimensional form. The wave excitation forces and moments are presented in Appendix B in the nondimensional form described earlier.

Static Experiments

The statics values are presented in Figures 8 and 9. Figure 8 gives the variation of the equilibrium heave height for design displacement with angle attack for the speeds and fan configurations that were investigated. It is interesting to note that the height variation shows

16

great differences between standstill and underway speeds. In this case, heave was positive down to agree with the chosen coordinate systems. Zero heave represented the point where the sidewall amidships was just touching the water. It can be noted that the model rode higher (lower h value) for the 2-3-2 fan configuration as was expected. As the speed became greater, dynamic effects on the sidewalls and seals increased in importance; thus the slopes of the curves became more negative.

The variation of pitch moment with angle of attack is given in Figure 9. The curves all show a strong restoring tendency indicating positive static pitch stability. The amount of stability does not change appreciably with speed.

Oscillation Experiments

Oscillation experiments were conducted at 6, 9, and 12 knots for the 2-0-2 fan configuration and at 12 knots for the 2-3-2 fan configuration. So that sidewall contributions to the stability derivatives could be determined, oscillations were made at 9 knots with the fans off and seals taped.

Tables 2 and 3 contain the dimensional values of the stability derivatives obtained from the heaving and inertial pitching oscillation techniques, utilizing the data analysis approach described in this report.

The sidewall-only oscillations are given in Figures 10 through 17. To simplify comparisons, the model was placed at the equilibrium trim and heave appropriate for 9 knots at the 2-0-2 fan configuration. The data show good repeatability and not much scatter. The lines for determining derivatives go through almost all the points. The derivatives

17

for the sidewalls should behave like a surface ship since the cushion effects were not present. The terms are consistent with that expected for a surface ship. The Z_h and M_Θ buoyancy terms are large and negative. The $Z_{\dot{w}}$ and M_q (damping terms), are negative which indicate positive damping. The $M_{\dot{q}}$ (added moment of inertia), is positive which is unusual but it is small compared to I_y. There was no body axes pitching conducted for the sidewalls alone.

The results of the 2-0-2 fan configuration oscillations are given in Figures 18 through 25. Figures 18, 19, 20 and 21 represent the results for heaving oscillations. The data is consistent for the three frequencies, but the limited number of frequencies makes the determination of slope and intercept very difficult. Large errors can result from one or two bad points or scatter. Figure 20, for 6 knots, illustrates these problems, showing that any curve fit is a compromise. In Figures 16 and 18, the intercepts agree for the most part with the static results for Z_h and M_h giving reasonable confidence in the data.

Figures 22, 23, 24, and 25 are from inertial pitch oscillations. The data shows an increase in inconsistency. The three points do not form good lines in some cases, particularly for the damping data in Figures 23 and 25. The data variations may be caused by frequency effects; however, there is not enough data to show trends. This inconsistency reveals the need for testing at many more frequencies, which can be done with the single strut pitch-heave oscillator.

The linear derivatives given in Table 2 are the result of the extrapolation and curve fit process. For the 2-0-2 fan configuration there are results at three speeds and the effect of speed can be ascer-

18

tained. As would be expected, the primary buoyancy terms Z_h and M_Θ
as well as M_h are not much affected by speed. Z_Θ does not increase with
speed which probably reflects the planing characteristics of the seals
thus increasing this coupled stiffness at the higher speeds. The term
$Z_{\dot{w}}$ is positive at all speeds (indicating negative added mass), and becomes
less positive at higher speeds. The heave damping terms are speed depen-
dent in their dimensional form. The "added moment of inertia" term, $M_{\dot{q}}$, is
initially negative at 6 knots but becomes positive at higher speeds. The
pitch damping and coupling terms vary nonlinearly with speed. The changes
with speed are to be expected as the Froude number is approaching a value
of one and the flow is changing substantially as speed increases.

A comparison between the sidewall derivatives and the 9 knot deriva-
tives for the 2-0-2 fan configuration is revealing. As might be expected,
the buoyancy terms are larger when the fans are operating. The $Z_{\dot{w}}$ changes
sign and becomes positive with a larger magnitude when cushion effects
are included. The heave damping terms Z_w and M_w increase greatly in
magnitude. The $M_{\dot{g}}$ also increases but the coupling terms $Z_{\dot{q}}$ and $M_{\dot{w}}$ remain
about the same. The pitch damping terms Z_q and M_q increase when the fans
operate but not as much as the heave terms do. It is apparent that the
sidewall dynamics for this surface effect ship influence pitch dynamics
strongly but are not as important in considering heave dynamics. This
suggests that a math model which based its pitch-heave predictions on
sidewall effects would be fairly good for pitch but very poor for heave.
Thus the effect of sidewall design on craft vertical plane dynamics should
be investigated more thoroughly and the cushion-water surface interactions
with the sidewalls should be emphasized in future math model developments.

19

The results of the 2-3-2 fan configuration heaving oscillations at 12 knots are given in Figures 26, 27, 28, and 29. The data is fairly good, but substantial scatter existed at the low frequencies. Since there was more cushion air flow, the forces being measured were higher for the most part than in the other oscillation experiments. The comparison of the 2-3-2 fan configuration results with the 12 knot 2-0-2 results reveals that "added mass" was increased, becoming considerably more positive (negative added mass effect) when the three plenum fans were added. M_w also increased in magnitude but the other terms did not change much. Thus the plenum fans influenced the acceleration dependent terms but not the rate dependent heave terms.

Wave Excitation Experiment

The results of the wave excitation experiments are presented in nondimensional form in Appendix B. Regular wave excitation data was obtained at two speeds, 9 and 12 knots. The transient technique was applied at 6, 9, and 12 knots.

The 6 knot transient results are given in Figures 30 to 33 where heave exciting force, heave phase angle, pitch exciting moment and pitch phase angle are presented. The quantities are plotted against nondimensionalized encounter frequency. The results for 6 knots are consistent with the exception of the pitch exciting moment, Figure 32. Even this figure indicates the data trends clearly. The heave-exciting force is fairly constant with the heave phase angle, approaching 180° as it should for zero frequency and the current sign convention. Pitch exciting moment seems to have a null point at about $\mu_e = 4.5$. Confidence in the accuracy of the transient wave data is enhanced by

20

the good correlation with regular wave results at the other speeds. The range of encounter frequencies is limited by the capabilities of the wavemaker system.

The results for 9 knots are given in Figures 34, 35, 36, and 37. These figures show regular and transient wave results plotted together. The correlation is excellent and the scatter is minimal up to an encounter frequency, μ_e of 8. Beyond this point the transient results show some scatter but duplicate all the trends of the regular wave results. The agreement between the techniques gives a high level of confidence in the results. Figures 36 and 37 show the potential of the transient wave techniques for determining excitations. The data shows the null point at $\mu_e = 7$ very clearly. The additional detailed information from the transient wave defines the phase shift very closely. The transient points at low frequency in Figure 37 indicate that the pitch moment phase extrapolated to 270° as was expected, (a 90° lead on the heave force phase). The transient waves results produced more information than the regular waves in the time it took to do one or two discrete frequency regular wave runs.

The 12 knot results for both techniques are presented in Figures 38-41. The correlation between the techniques and the consistency of the data are good in all cases. A null point in pitch exciting moment at $\mu_e = 8$ is very apparent. Figures 39 and 41 indicate that the scatter in the transient data is not much greater than the scatter that would have appeared in the regular wave data, had a comparable number of data points been taken.

21

The wave excitation data can be combined with the stability deriva-
tives in a frequency domain simulation to provide predictions of the craft
motions which are based on experimental results. These predictions can
then be compared with free model motion results.

CONCLUSIONS AND RECOMMENDATIONS

1. The body axes pitching definition (as employed in submarine re-
search) is not suitable for determining the pitch dynamics of air cushion
supported craft. The changes in immersion of the craft associated with
this type of pitching introduce large variations in buoyancy forces that
dominate over the measured quantities, leading to inaccuracies and incon-
sistencies.

2. The water-fixed axes, (inertial) pitching technique that employs
a 180° phase between the fore and aft strut motion (or one moving piston
and a fixed point at the CG) will provide meaningful results that can
be converted to the usual body axis defined stability derivatives.

3. The sidewalls of a high length-to-beam ratio SES contribute
significantly to the pitch dynamics but do not affect significantly the
heave terms in the equations of motion. More work in sidewall design
and cushion interaction effects in the vertical plane is recommended.

4. The inclusion of plenum fans in the XR-5 model tends to make
the acceleration-dependent terms increase in magnitude while hardly
affecting the rate dependent terms in heave.

5. Conclusions on the motion characteristics of the XR-5 model
based on these results and any indication of the validity of the results
must await a simulation effort which is currently underway.

22

6. The transient waves approach can be utilized to determine the wave excitation forces and moments over the entire frequency range as accurately as the much more time consuming and expensive regular wave technique. The force and moment response of the block gages to the transient wave is much faster than a motion response would be, thus the technique can be applied more generally than the free model transient waves technique. In addition, the current state-of-the-art in data analysis permits on-carriage analysis of the transient results for the entire frequency range. In light of these results and system improvements, it is recommended that the transient technique be investigated further and that transient oscillation experiments, as developed in Reference 7, also be investigated as a means of improving the efficiency of the Navy's experimental techniques.

ACKNOWLEDGMENTS

REFERENCES

1. Magnuson, A.H. and K.K. Wolff, "Seakeeping Characteristics of
the XR-5, A High Length-to-Beam Ratio Manned Surface Effect Testcraft:1.
XR-5 Model Response in Regular Head Waves." SPD Report 161-01, March 1975.

2. Gertler M., "The DTMB Planar Motion Mechanism System", Symposium
on Towing Tank Facilities, Instrumentation and Measuring Techniques,
Zagreb, 1959.

3. Davis, M.C. and E.E. Zarnick, "Testing Ship Models in Transient
Waves", Fifth ONR Symposium on Naval Hydromechanics, Bergen, 1964.

4. Gersten, A., "Notes on Ship Model Testing in Transient Waves",
NSRDC Report 2960, April 1969.

5. Goodman, A., "Experimental Techniques and Methods of Analysis
Used in Submerged Body Research", Third ONR Symposium on Naval Hydromechanics, 1960.

6. Comstock, J.P., (Ed.), Principles of Naval Architecture, SNAME,
1967.

7. Smith, W.E. and W.E. Cummins, "Force Pulse Testing of Ship Models",
Fifth ONR Symposium of Naval Hydromechanics, 1964.
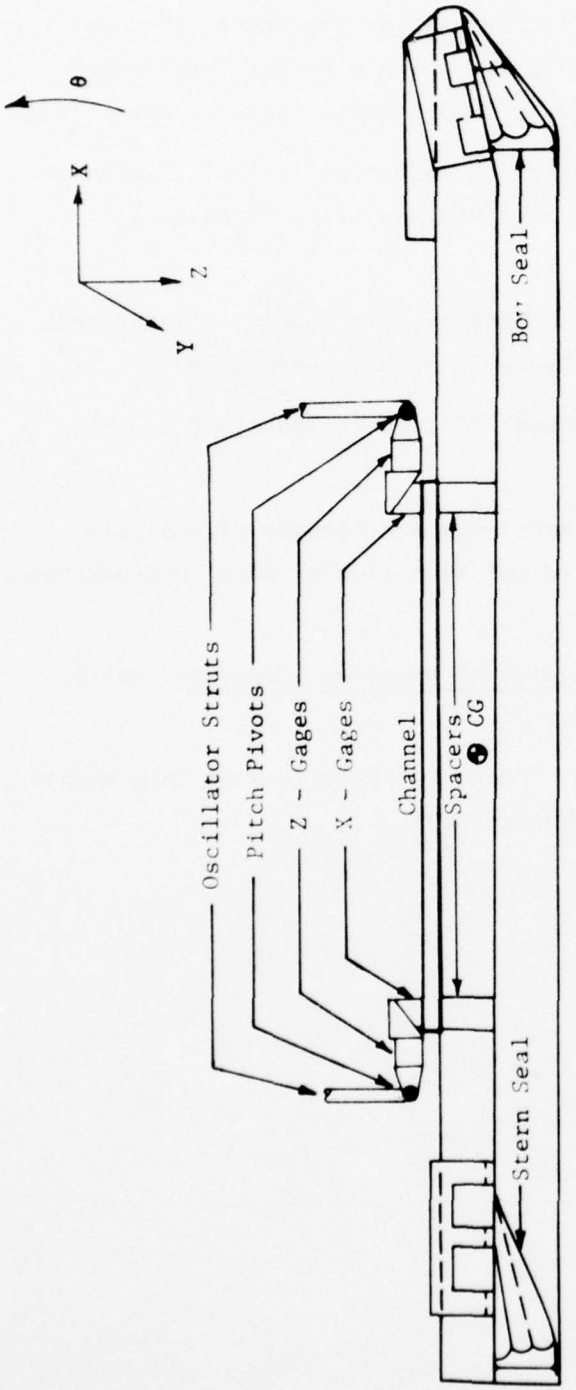
INBOARD PROFILE VIEW
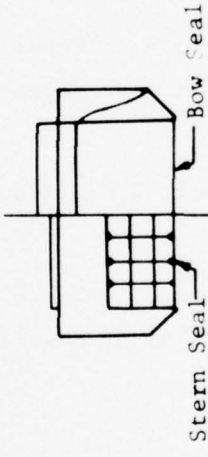
OUTBOARD
BODY VIEW

Figure 1 - XR-5 Model as Tested and Positive Coordinate
Directions

26
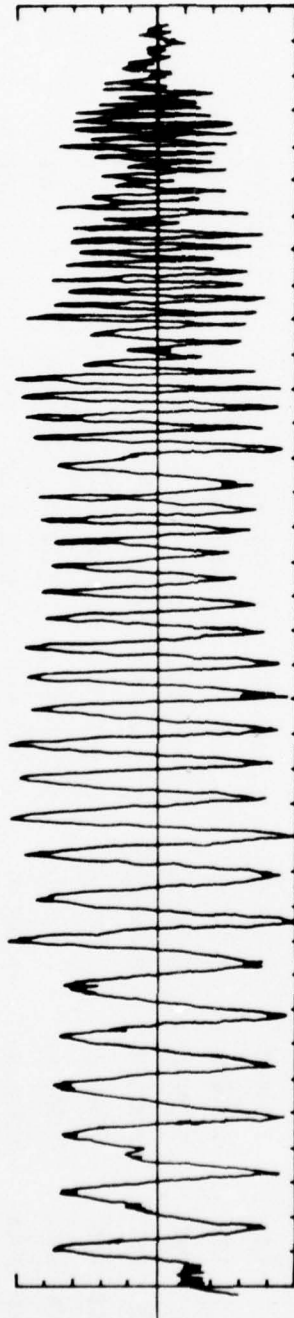
Figure 2 - Wave Height Data for Transient Waves Encountered
at a Speed of 12 Knots

27

CARRIAGE II   ROTARY COEFFICIENTS   JANUARY 1975

RUN NO 700

RECORDS: 1 - 71
TIME: 0.000 - 28.250 SEC

TE = 5.650 SEC   CARVEL = 8.932 FTS   WE = 1.112 RAD/SEC

CHAN		CALIB	MEAN	ROOT00	AMP	PHASE	IN-PHASE	OUT-OF-PHASE
2	REFRNC IN	1.00E 00	-9.02E-03	8.728E-01	8.703E-01	0.0	8.703E-01	0.000E 00
3	STRUT F IN	3.33E-01	-4.99E-03	3.309E-01	3.308E-01	3.3	3.295E-01	-1.900E-02
4	STRUT A IN	3.33E-01	3.00E-03	3.243E-01	3.238E-01	2.9	3.234E-01	-1.632E-02
5	ZFWD LBS	4.00E 01	6.72E 01	7.705E-01	2.559E 00	10.2	2.515E 00	-4.746E-01
6	ZAFT LBS	4.00E 01	4.17E 01	5.832E 00	5.219E 00	8.1	5.168E 00	-7.315E-01
7	XFWD LBS	1.60E 01	-4.10E 00	1.941E 00	7.468E-01	-94.8	-6.289E-02	7.441E-01
8	XAFT LBS	1.00E 01	-7.13E 00	4.183E 00	1.486E 00	35.5	1.209E 00	-8.634E-01
9	CUSH1 PSI	3.33E-01	7.76E-02	2.508E-03	1.039E-03	-108.1	-3.234E-04	9.872E-04
10	CUSH2 PSI	3.33E-01	2.44E-02	3.274E-03	1.191E-03	-86.2	7.907E-05	1.188E-03
11	ZFORCE LBS	4.00E 01	1.09E 02	6.097E 00	7.777E 00	8.8	7.685E 00	-1.191E 00
12	XFORCE LBS	1.00E 01	-1.12E 01	5.788E 00	1.152E 00	5.9	1.146E 00	-1.176E-01
13	PITMOM FTLB	1.60E 02	-1.02E 02	1.357E 01	1.066E 01	5.4	1.061E 01	-1.003E 00

28

Figure 3 - Computer Output from Oscillation Run
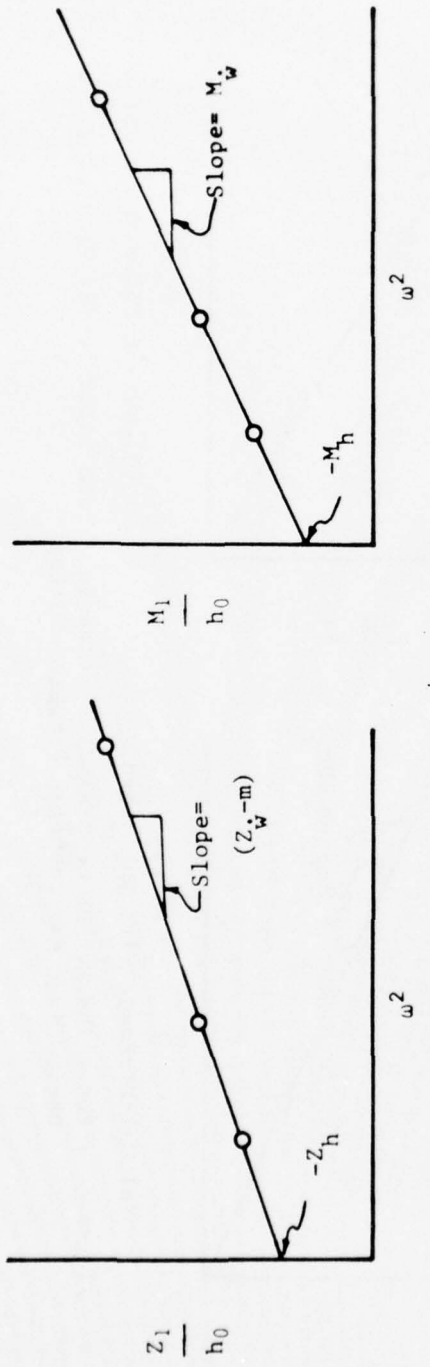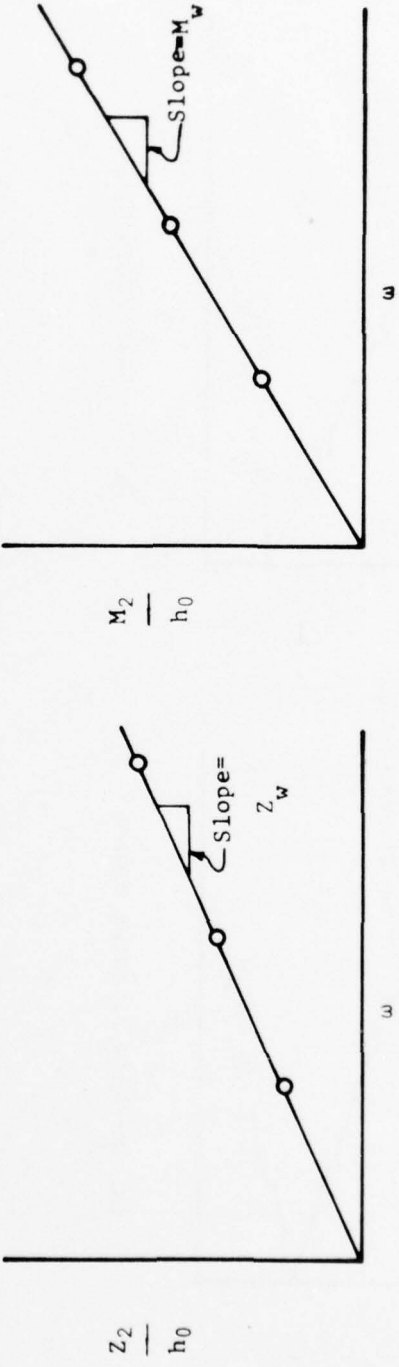
Figure 4 - Force and Moment Components Plotted in a Form Suitable for Obtaining Stability
Derivatives for Heaving Motion

29

(a) In-Phase Pitching Moment

(b) In-Phase Heave Force

(c) Out-of-Phase Pitching Moment

(d) Out-of-Phase Heave Force
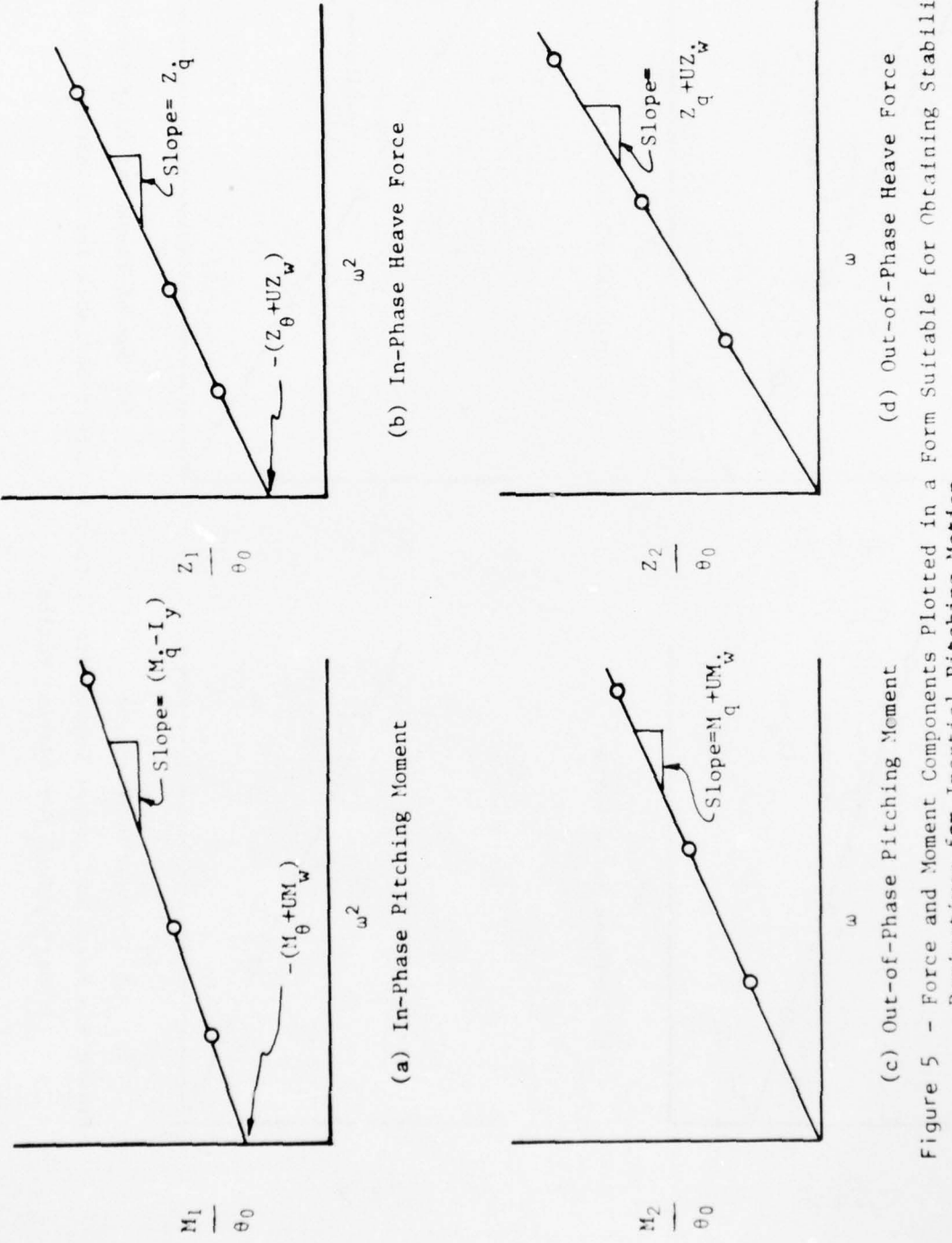
Figure 5 – Force and Moment Components Plotted in a Form Suitable for Obtaining Stability Derivatives for Inertial Pitching Motion
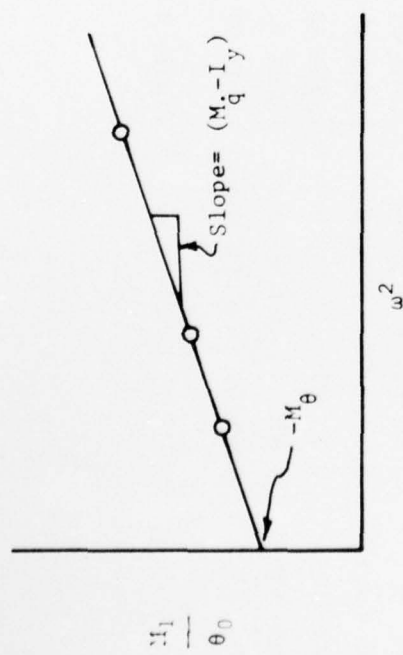
30

(a) In-Phase Pitching Moment
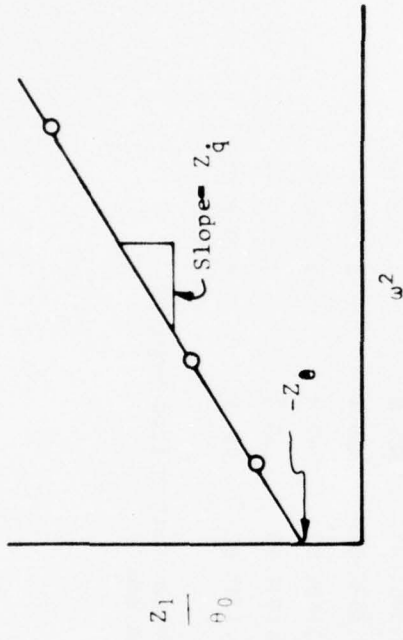
(b) In-Phase Heave Force
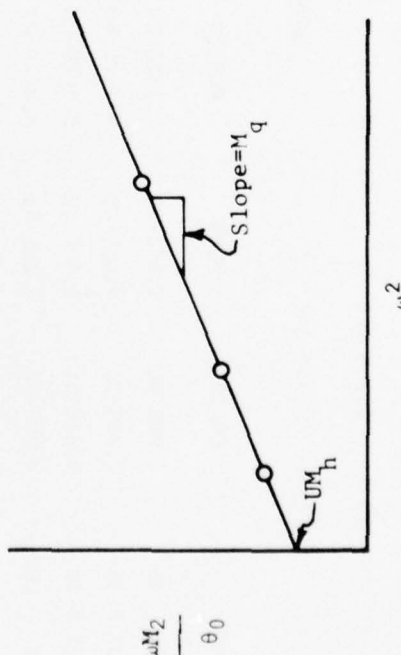
(c) Out-of-Phase Pitching Moment
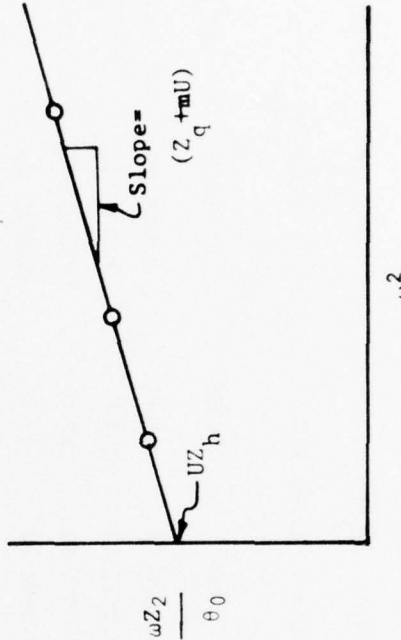
(d) Out-of-Phase Heave Force

Figure 6 – Force and Moment Components Plotted in a Form Suitable for Obtaining Stability
Derivatives for Body Axis Pitching Motion

31

CARRIAGE II   ROTARY COEFFICIENTS   JANUARY 1975

RUN NO 814

TE = 8.450 SEC   CARVEL = 8.933 KTS   UE = 13.963 RAD/SEC

TO = 1.398 SEC   LAMBDA = 18.885 FT   UO = 4.495 RAD/SEC

FE = 2.222 CPS   WAVE SLOPE = 3.245 DEG   CELER = 7.158 FPS

CHAN	CALIB	MEAN	ROOTOO	AMP	PHASE	IN-PHASE	OUT-OF-PHASE
2 REFRNC IN	1.00E 00	6.99E-02	1.136E 00	1.082E 00	0.0	1.082E 00	0.000E 00
3 STRUT F IN	3.33E-01	4.68E-03	9.430E-04	4.013E-04	234.8	-2.314E-04	3.279E-04
4 STRUT A IN	3.33E-01	1.38E-02	8.177E-04	1.851E-05	225.9	-1.289E-05	1.328E-05
5 ZFWD LBS	4.00E 01	3.05E 01	8.411E 01	7.265E 01	143.7	-5.858E 01	-4.296E 01
6 ZAFT LBS	4.00E 01	3.68E 01	5.799E 01	4.418E 01	144.2	-3.582E 01	-2.585E 01
7 XFWD LBS	1.00E 01	-4.09E 00	5.039E 00	1.781E 00	18.0	1.694E 00	-5.511E-01
8 XAFT LBS	1.00E 01	-1.15E 01	9.199E 00	1.683E 00	64.4	7.262E-01	-1.518E 00
9 CUSH1 PSI	3.33E-01	7.05E-01	2.415E-01	2.146E-01	301.8	1.132E-01	1.823E-01
10 CUSH2 PSI	3.33E-01	3.68E-01	2.819E-01	2.392E-01	328.4	2.038E-01	1.254E-01
11 ZFORCE LBS	4.00E 01	6.73E 01	1.406E 02	1.168E 02	142.4	-9.253E 01	-7.132E 01
12 XFORCE LBS	1.00E 01	-1.56E 01	1.395E 01	3.181E 01	39.3	2.462E 01	-2.014E 00
13 PITMOM FTLB	1.60E 02	2.55E 01	1.327E 02	1.139E 02	320.5	8.784E 01	7.253E 01

Figure 7 - Computer Output from Regular Wave Run

APPENDIX A

(Figures 8 thru 29)

33
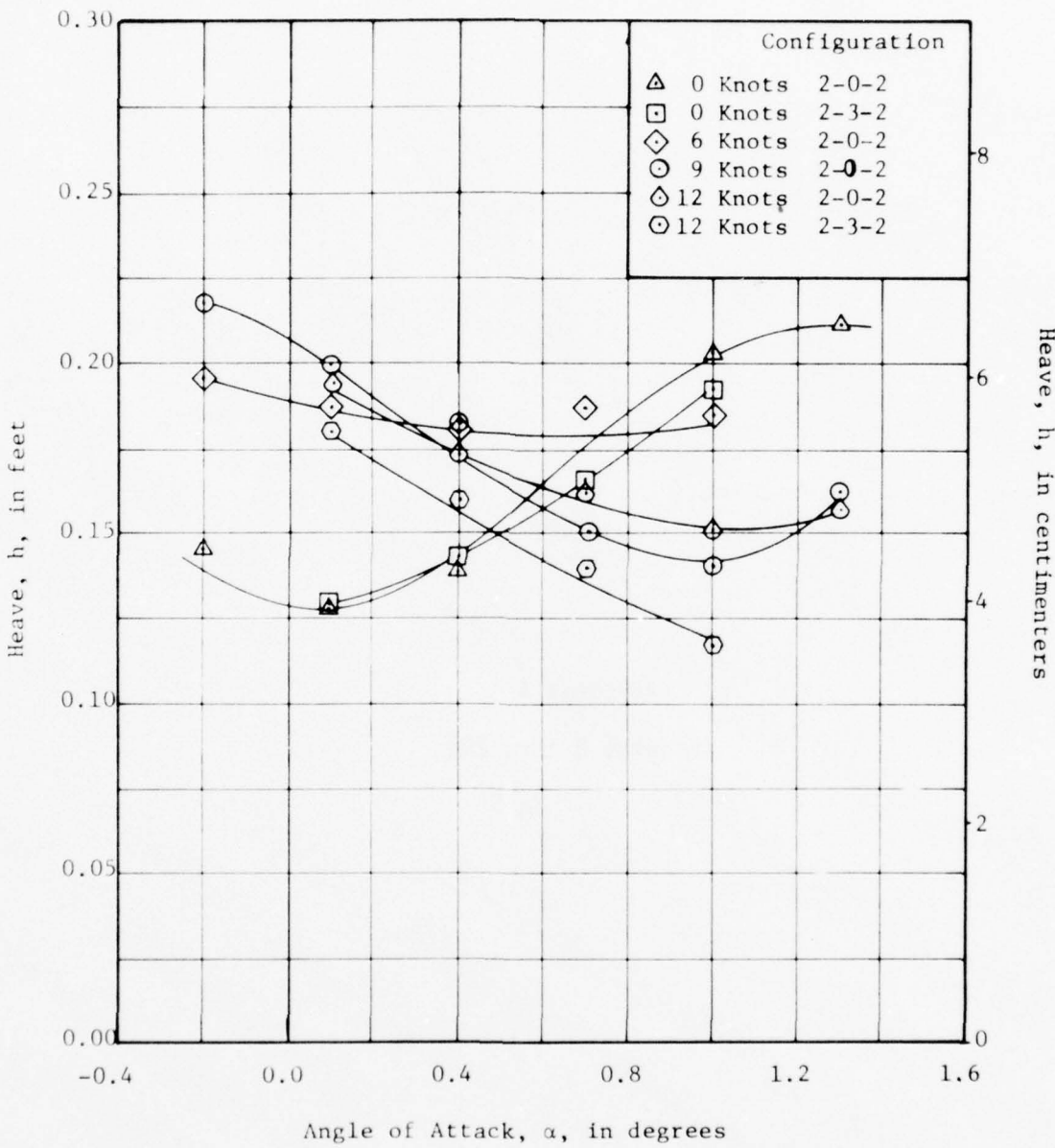
Figure 8 - Variation of Static Heave with Angle of Attack for a
Series of Speeds and Fan Configurations

34
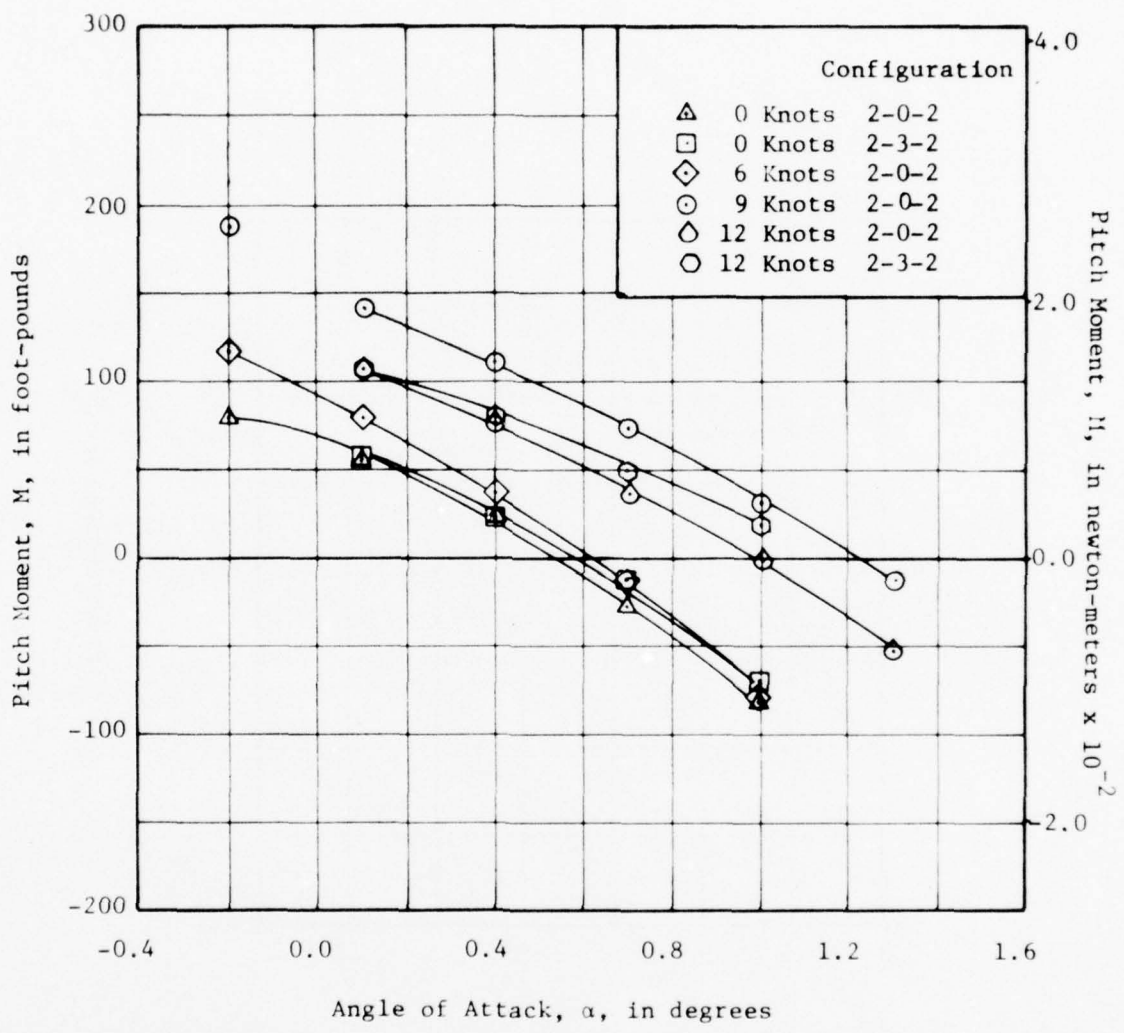
Figure 9 -Variation of Static Pitch Moment with Angle of
Attack for a Series of Speeds and Fan Configurations
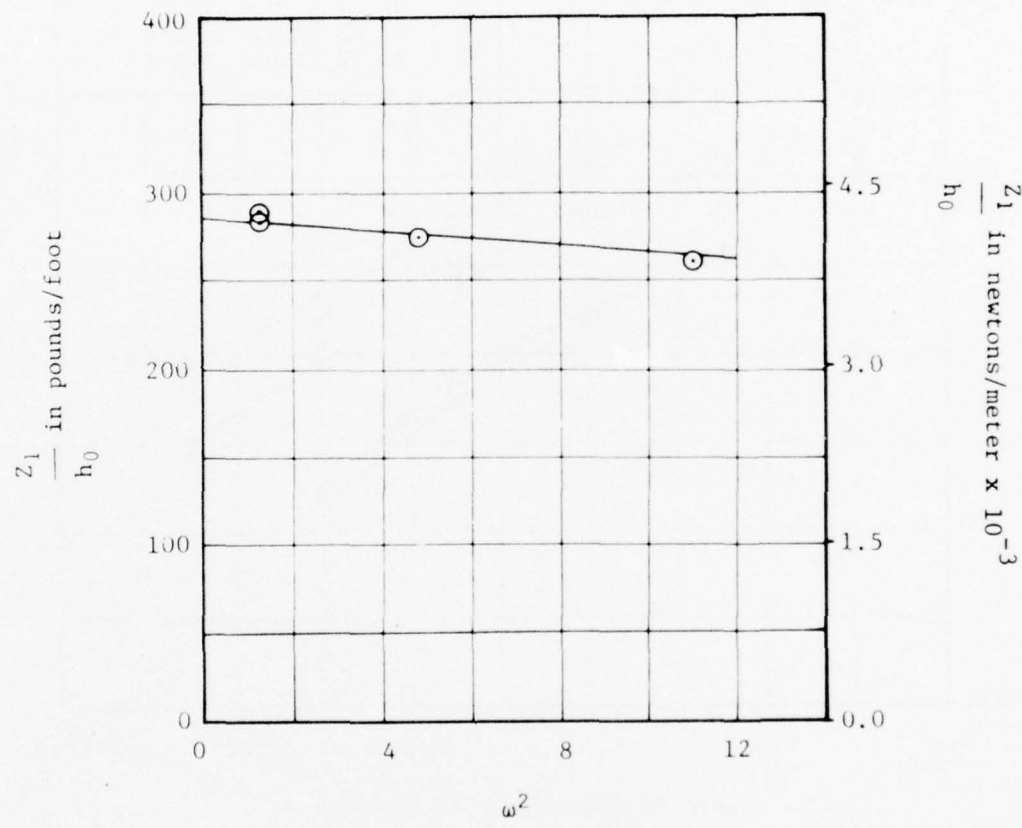
Figure 10 - Variation of In-Phase Heave Force with Frequency
Squared for Sidewalls at 9 Knots by Heaving
Technique
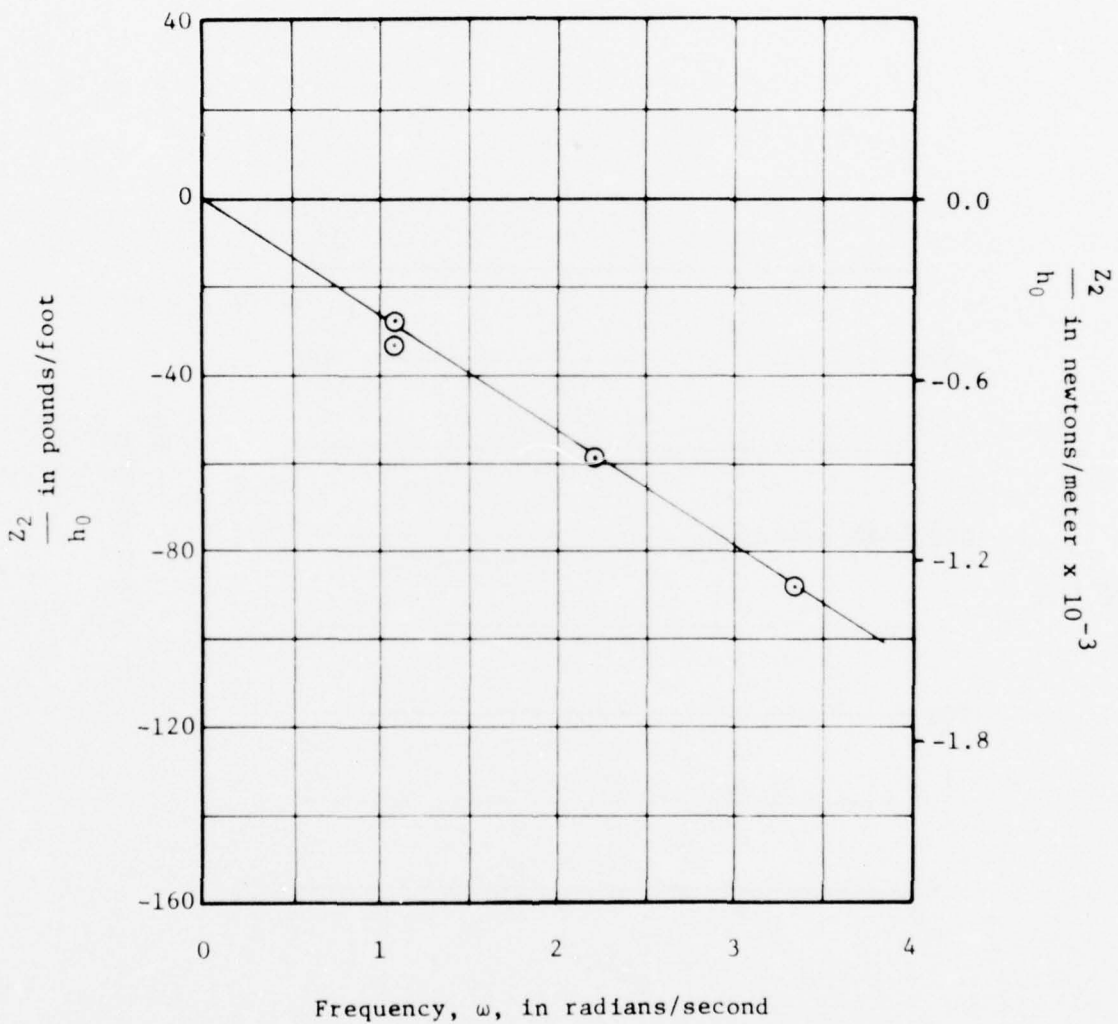
Figure 11 - Variation of Out-of-Phase Heave Force with Frequency for Siedwalls at 9 Knots by Heaving Technique

37
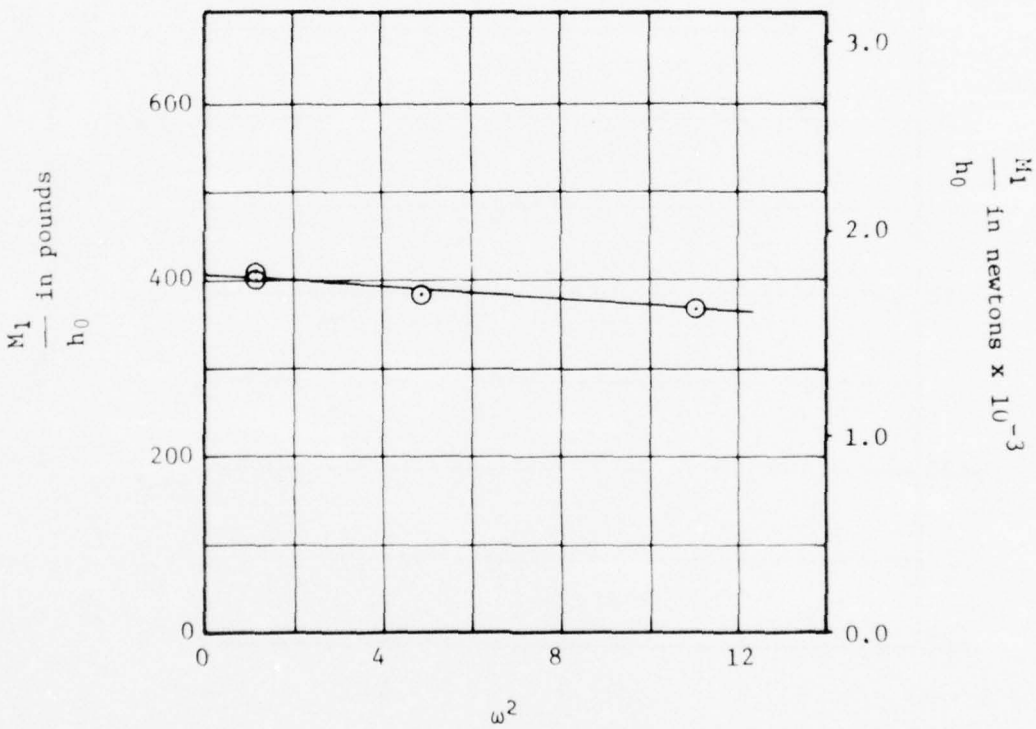
Figure 12 - Variation of In-Phase Pitch Moment with Frequency
Squared for Sidewalls at 9 Knots by Heaving
Technique
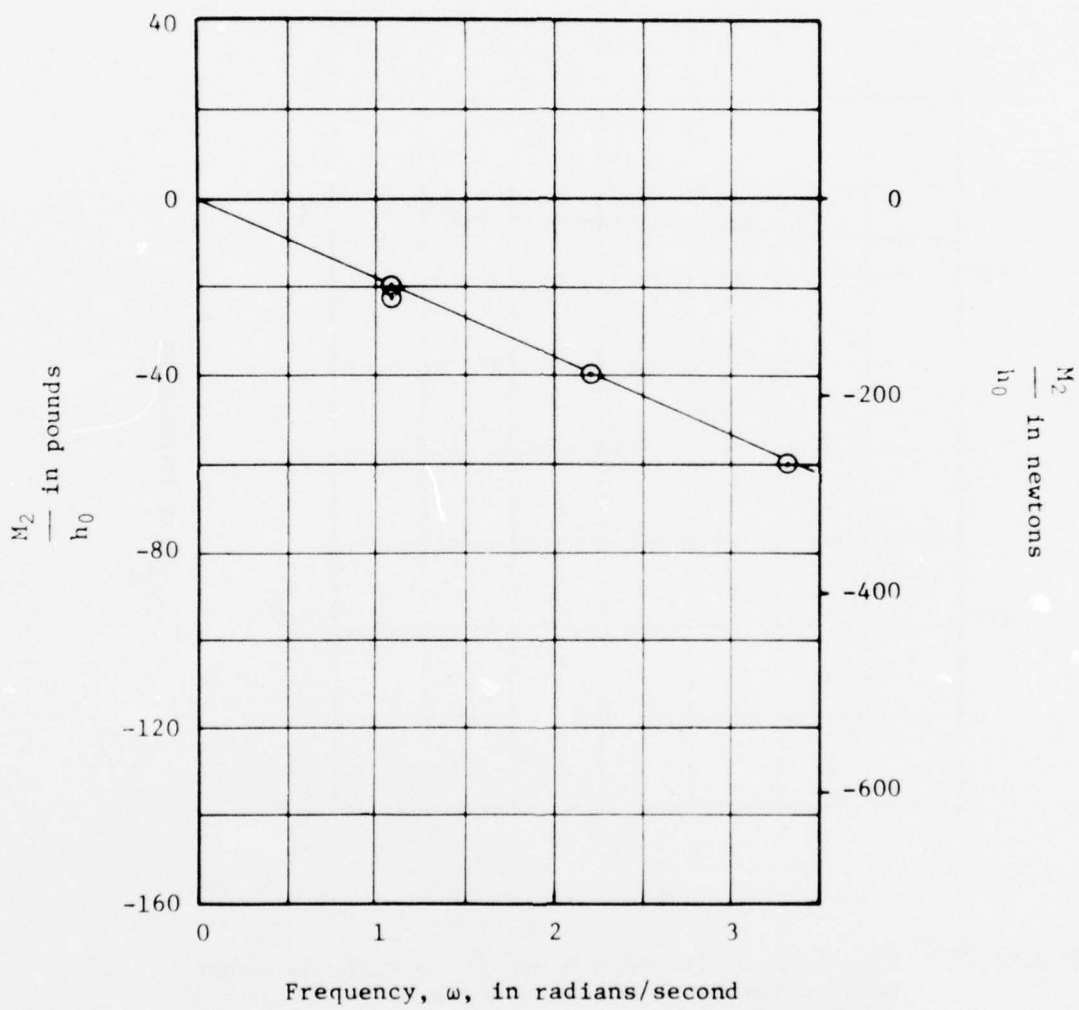
Figure 13 - Variation of Out-of-Phase Pitch Moment with
          Frequency for Sidewalls at 9 Knots by Heaving
          Technique
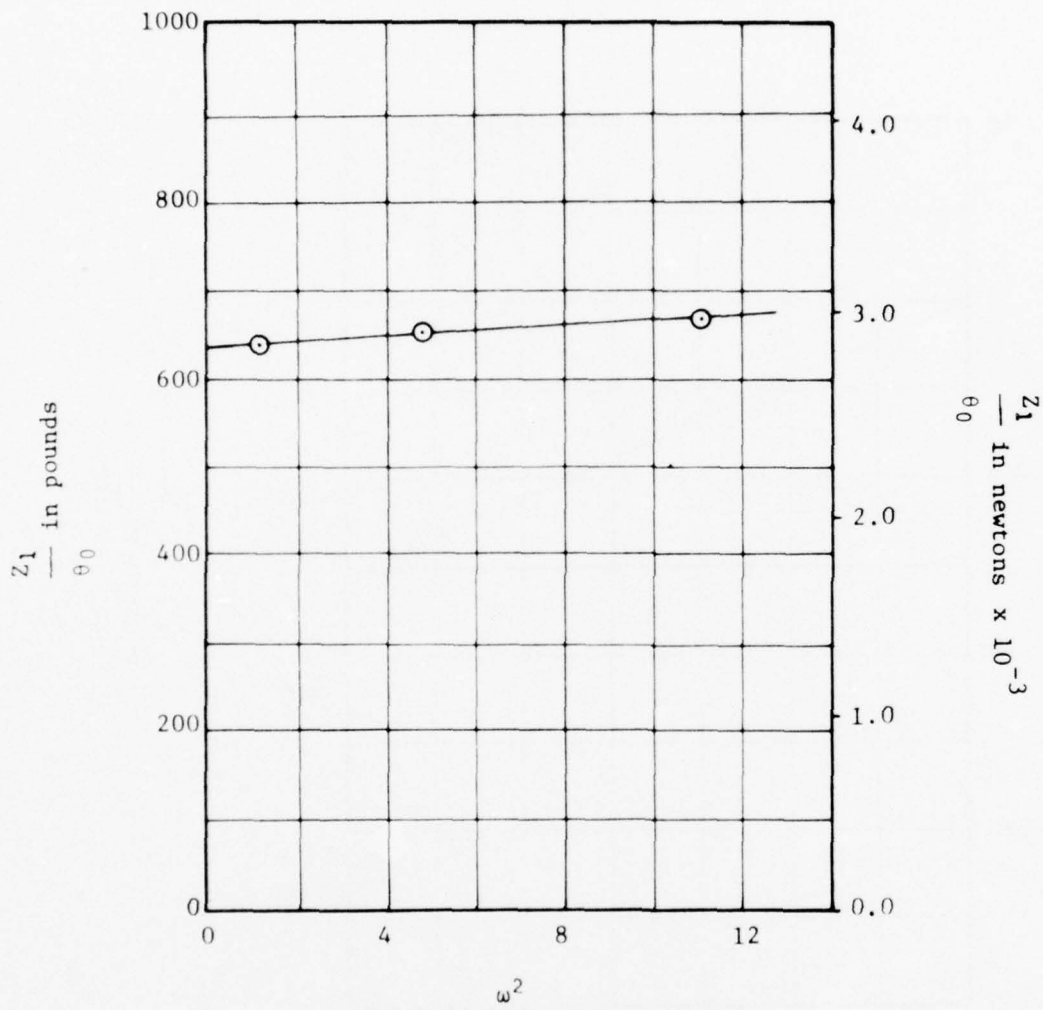
Figure 14 - Variation of In-Phase Heave Force with Frequency Squared for Sidewalls at 9 Knots by Inertial Pitching Technique
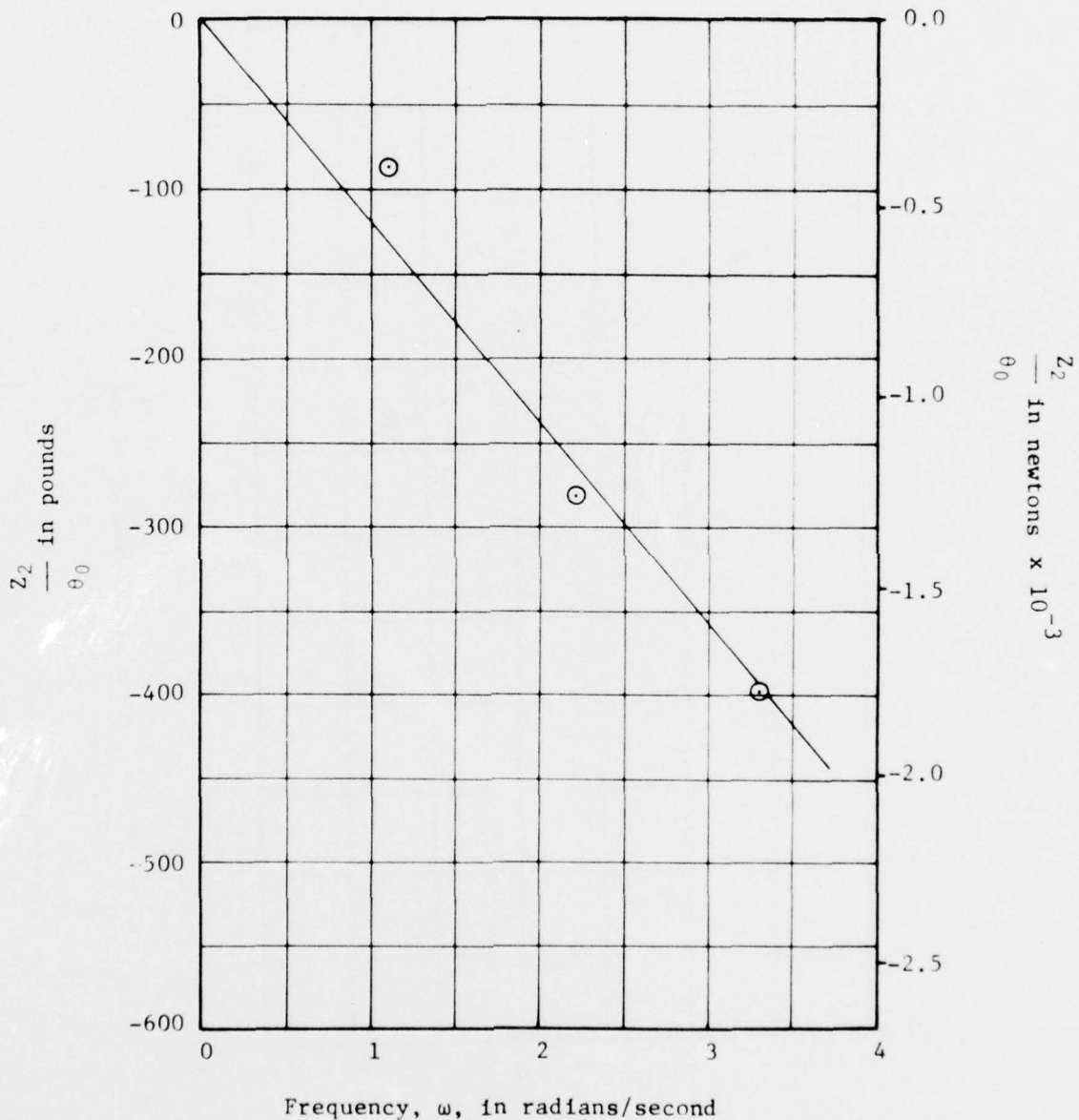
Figure 15 - Variation of Out-of-Phase Heave Force with Frequency for Sidewalls at 9 Knots by Inertial Pitching Technique

41
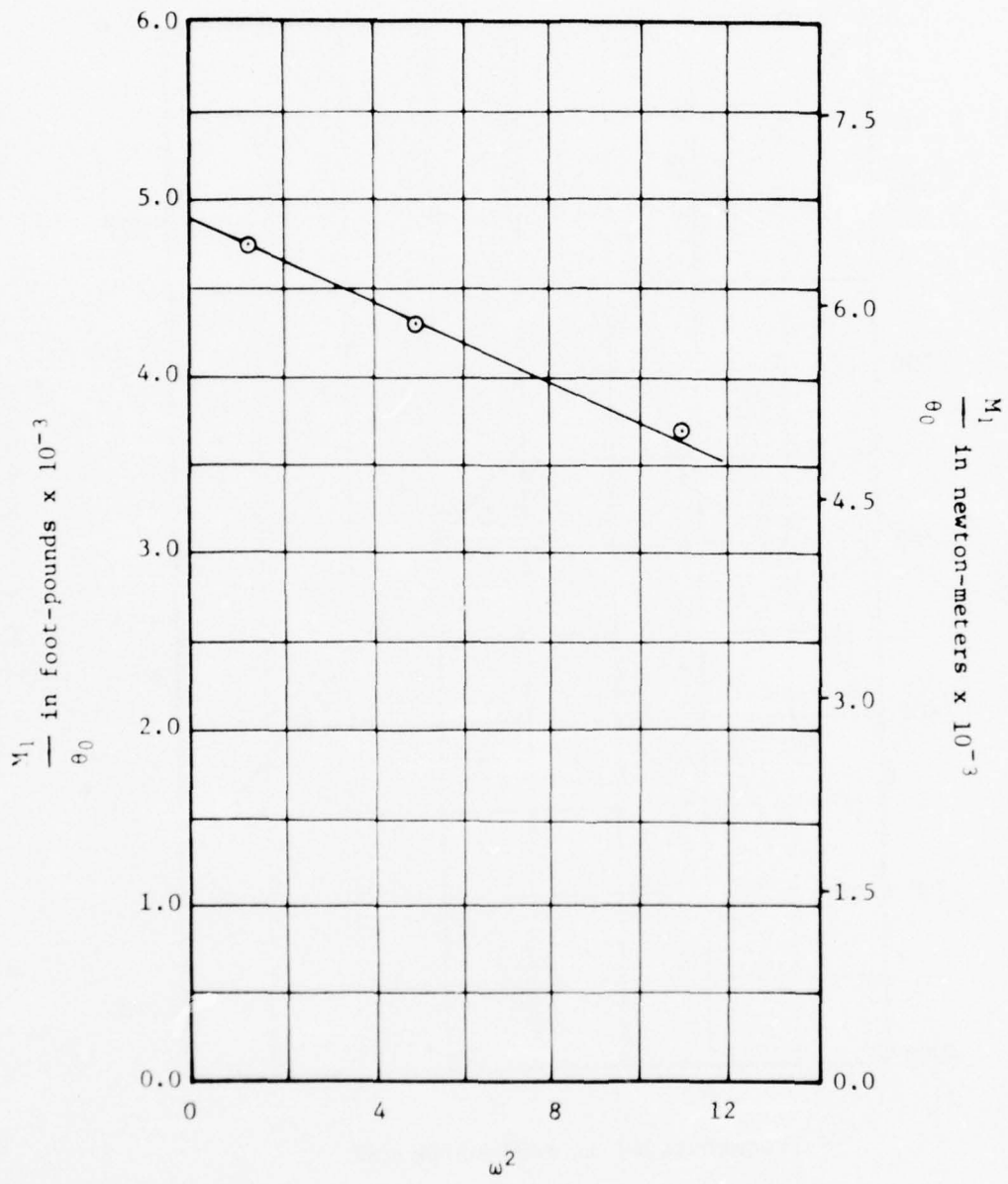
Figure 16 - Variation of In-Phase Pitch Moment with Frequency
Squared for Sidewalls at 9 Knots by Inertial Pitching
Technique
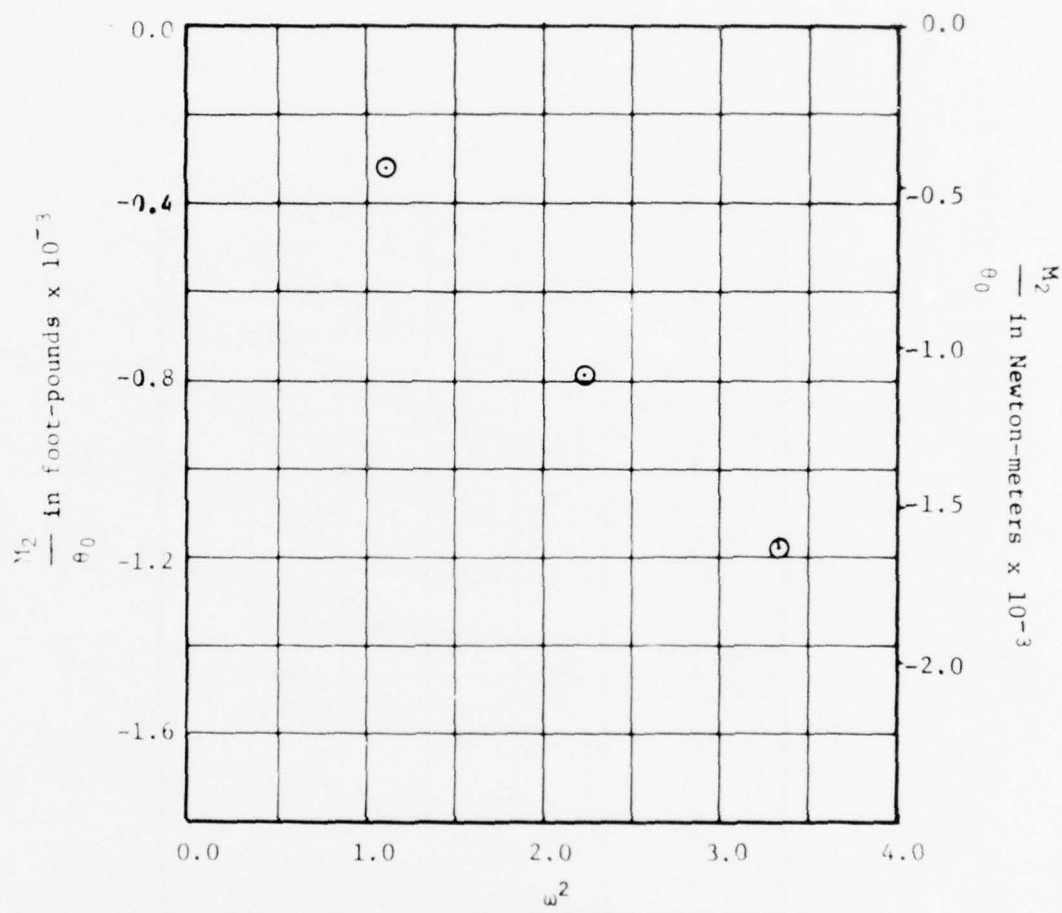
Figure 17 - Variaton of Out-of-Phase Pitch Moment with Frequency Squared for Sidewalls at a Speed of 9 Knots by the Inertial Pitching Technique

43
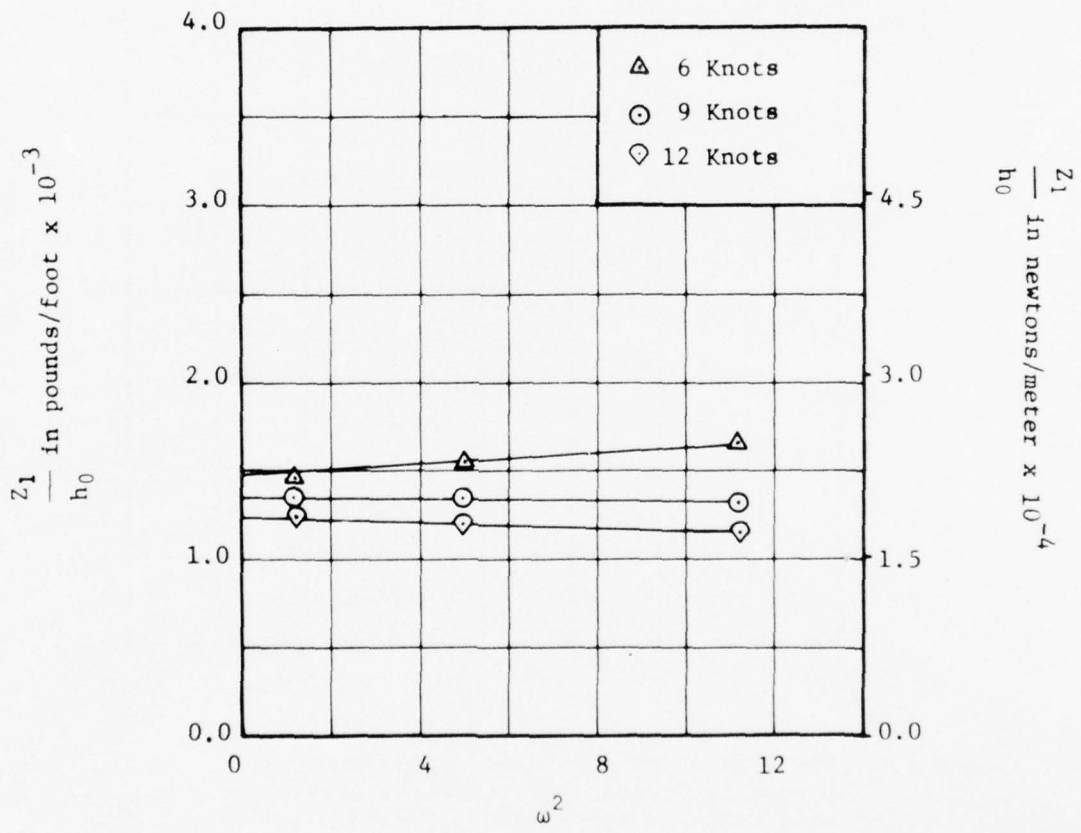
Figure 18 - Variation of In-Phase Heave Force with Frequency
Squared for a 2-0-2 Fan Configuration at a Series
of Speeds by Heaving Technique

44
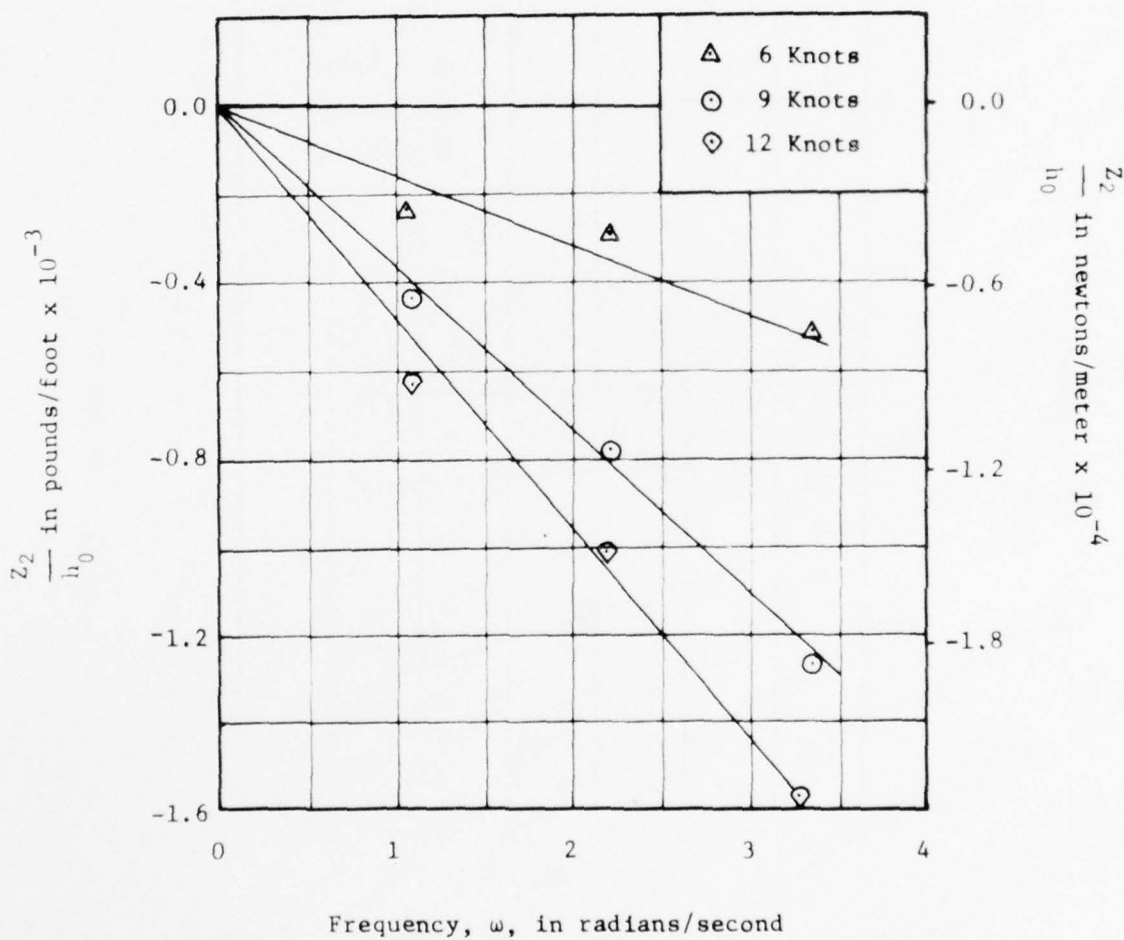
Figure 19 - Variation of Out-of-Phase Heave Force with
Frequency for a 2-0-2 Fan Configuration at
a Series of Speeds by Heaving Technique
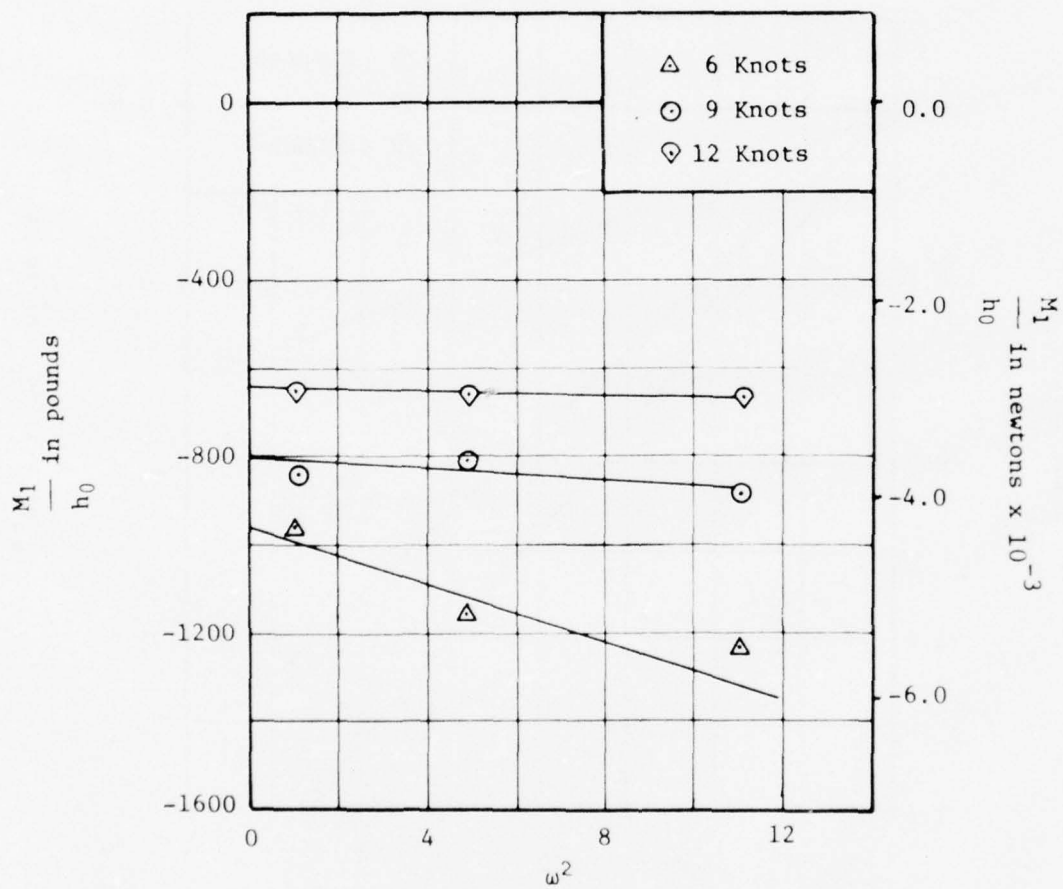
Figure 20 - Variation of In-Phase Pitch Moment with Frequency
   Squared for a 2-0-2 Fan Configuration at a Series
          of Speeds by Heaving Technique

46
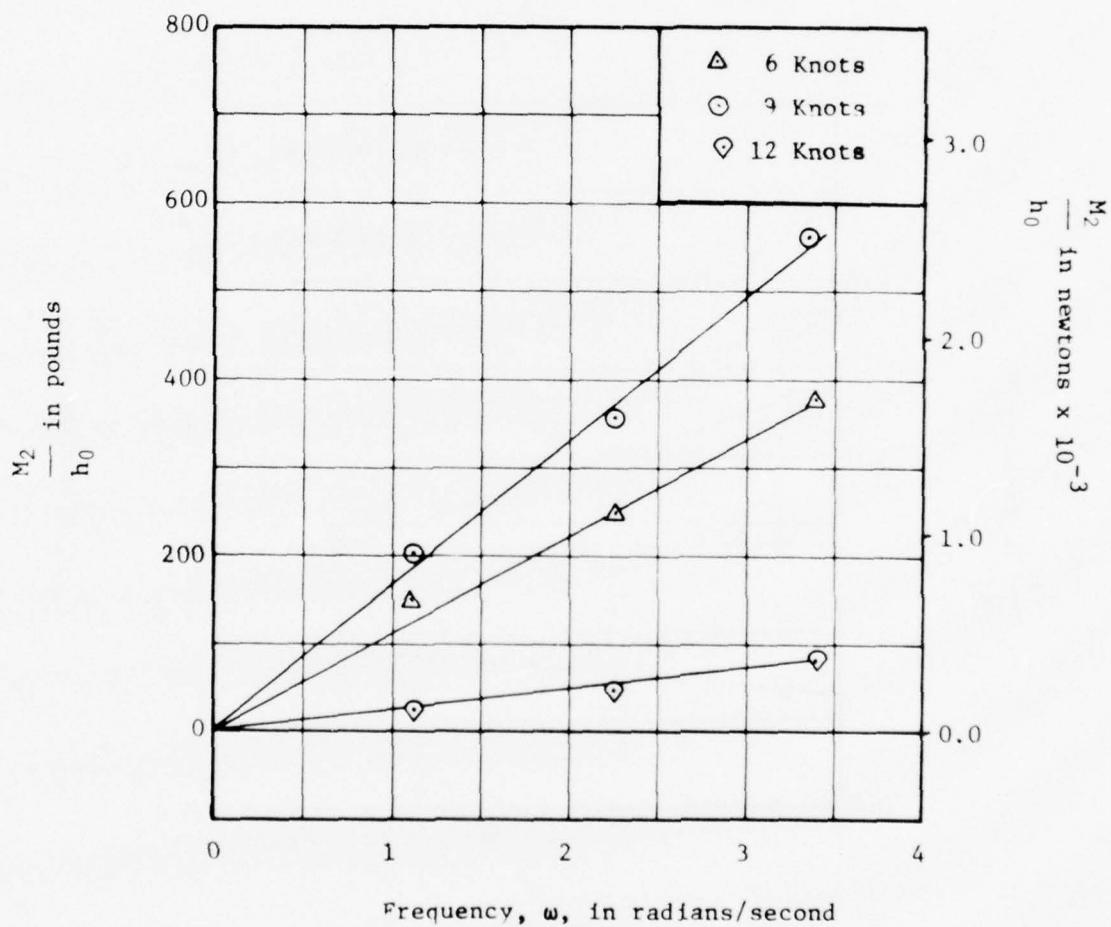
Figure 21 - Variation of Out-of-Phase Pitch Moment with
Frequency for a 2-0-2 Fan Configuration at
a Series of Speeds by Heaving Technique

47
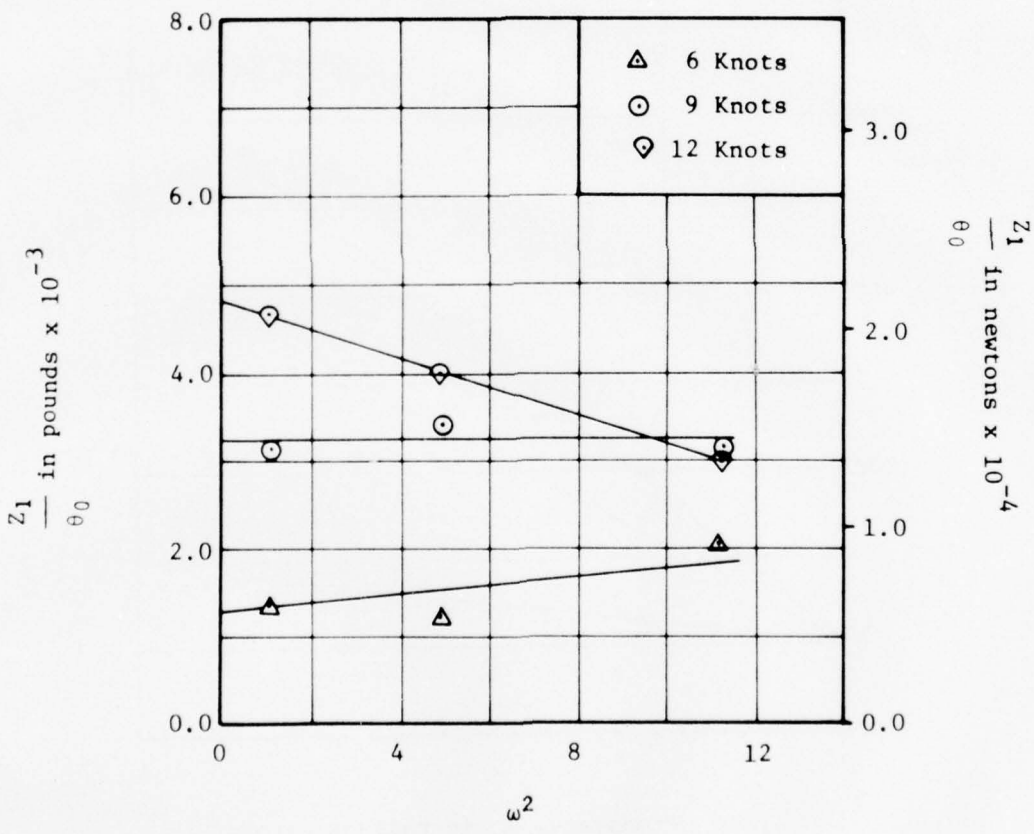
Figure 22 - Variation of In-Phase Heave Force with Frequency
Squared for a 2-0-2 Fan Configuration at a Series
of Speeds by Inertial Pitching Technique
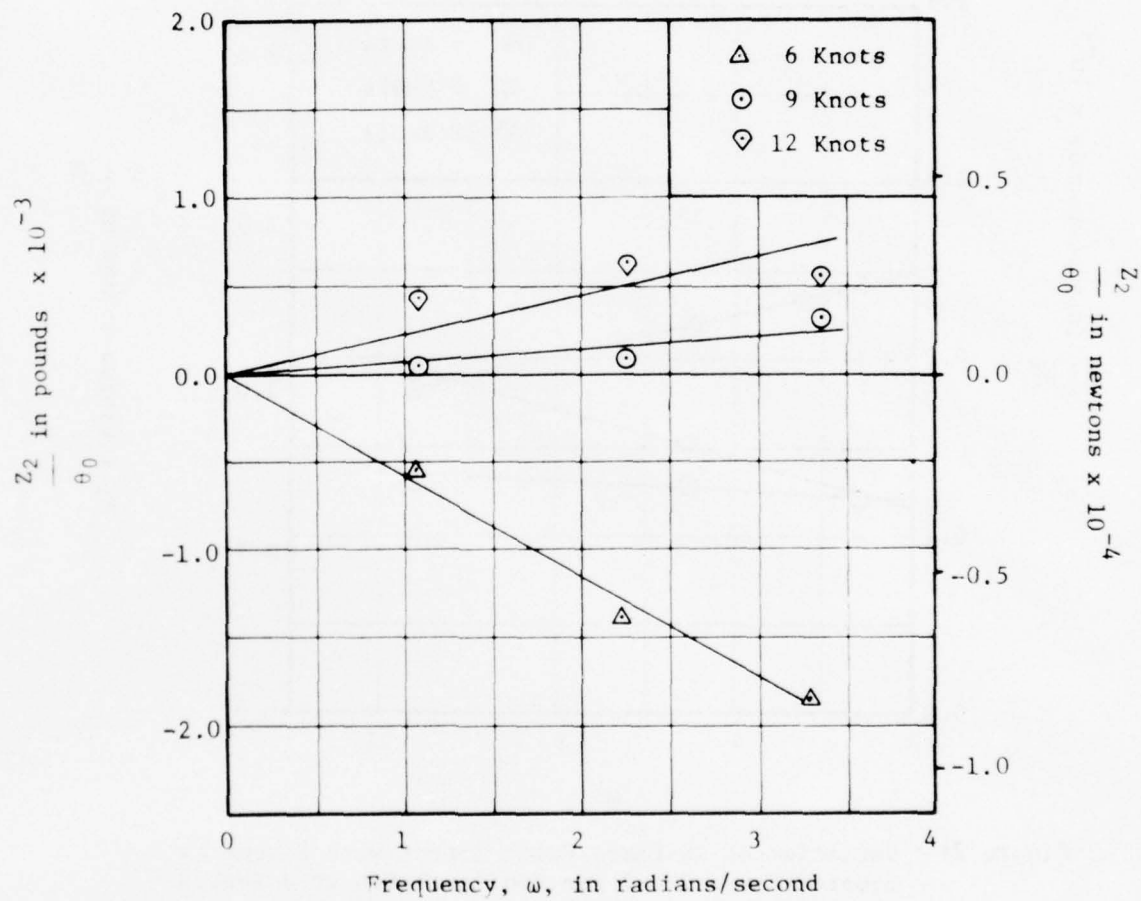
Figure 23 - Variation of Out-of-Phase Heave Force with
Frequency for a 2-0-2 Fan Configuration at
a Series of Speeds by Inertial Pitching Technique
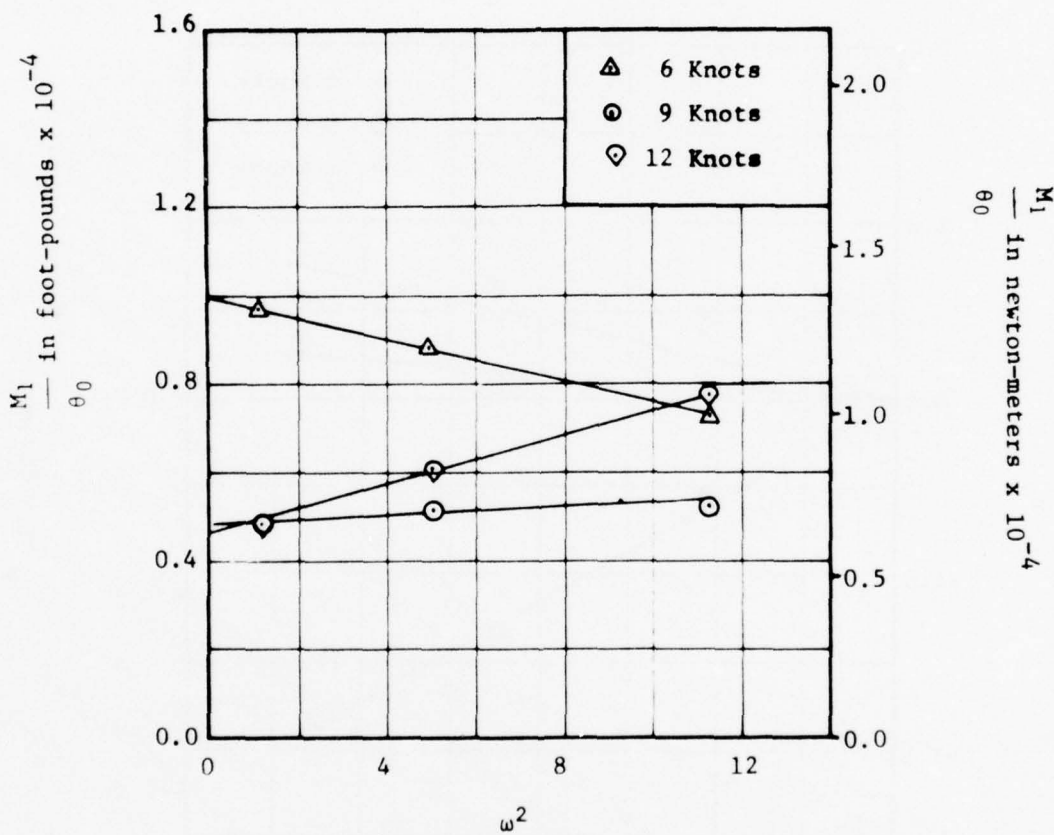
Figure 24 - Variation of In-Phase Pitch Moment with Frequency Squared for a 2-0-2 Fan Configuration at a Series of Speeds by Inertial Pitching Technique
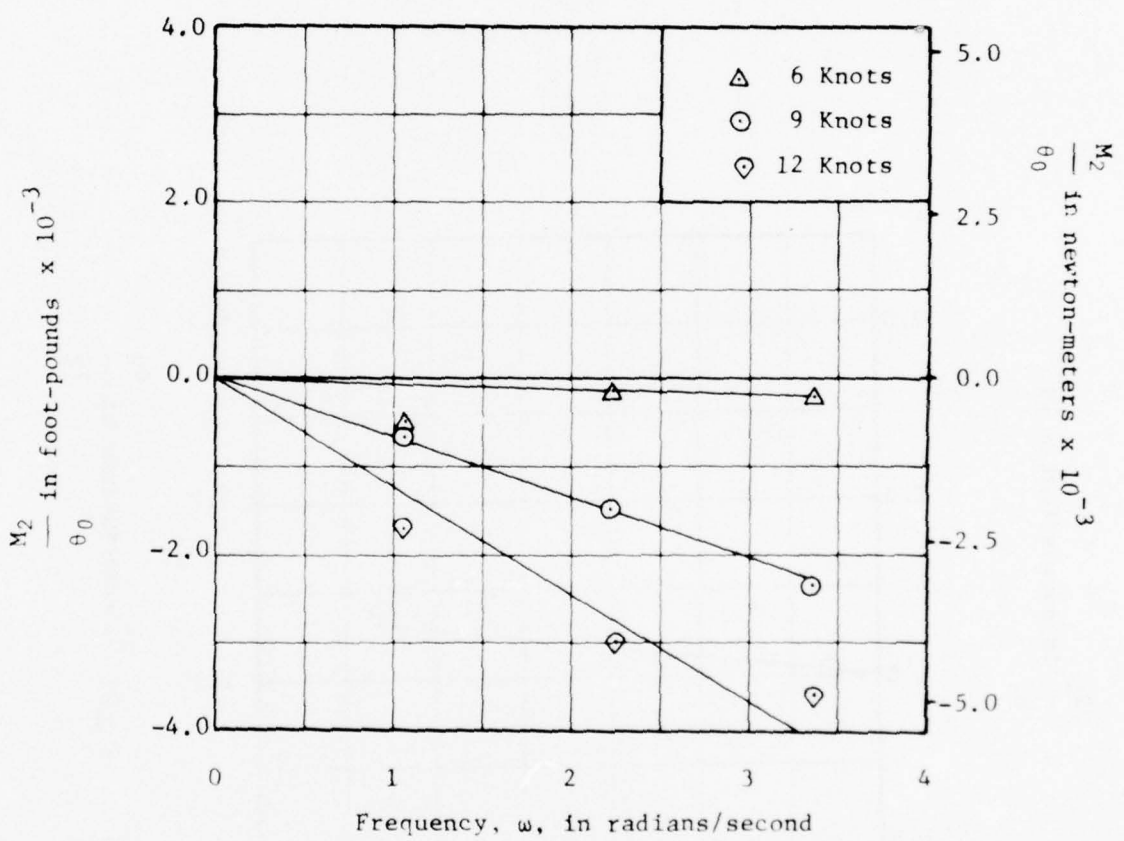
Figure 25 - Variation of Out-of-Phase Pitch Moment with
Frequency for a 2-0-2 Fan Configuration at
a Series of Speeds by Inertial Pitching Technique
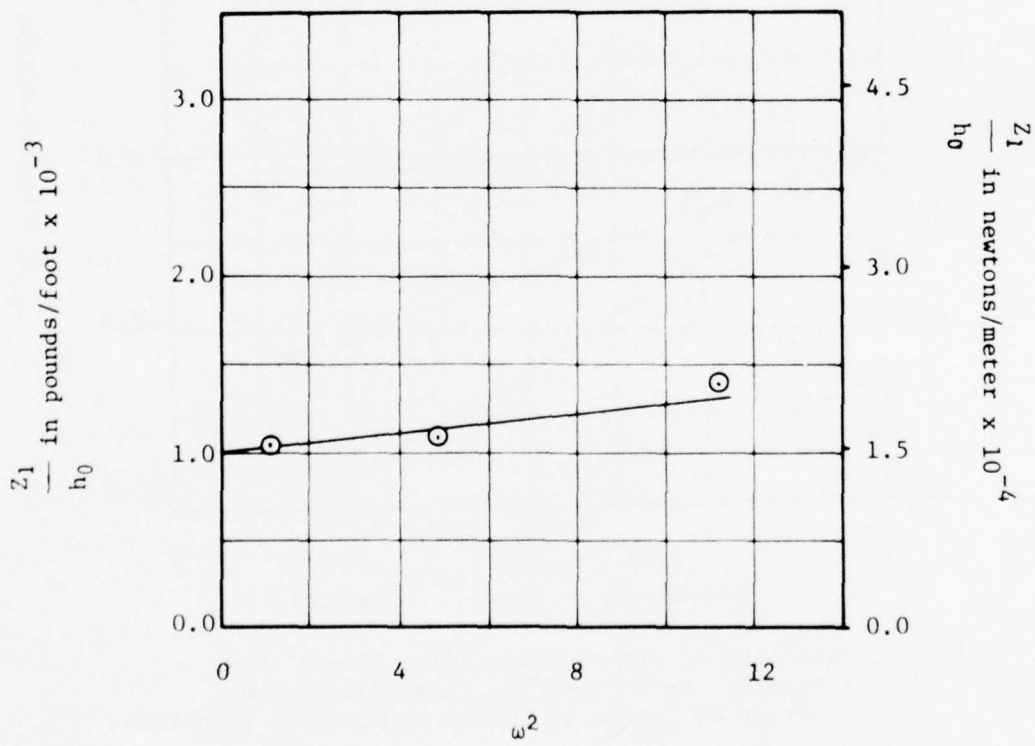
Figure 26 - Variation of In-Phase Heave Force with Frequency
Squared for a 2-3-2 Fan Configuration at 12 Knots
by Heaving Technique
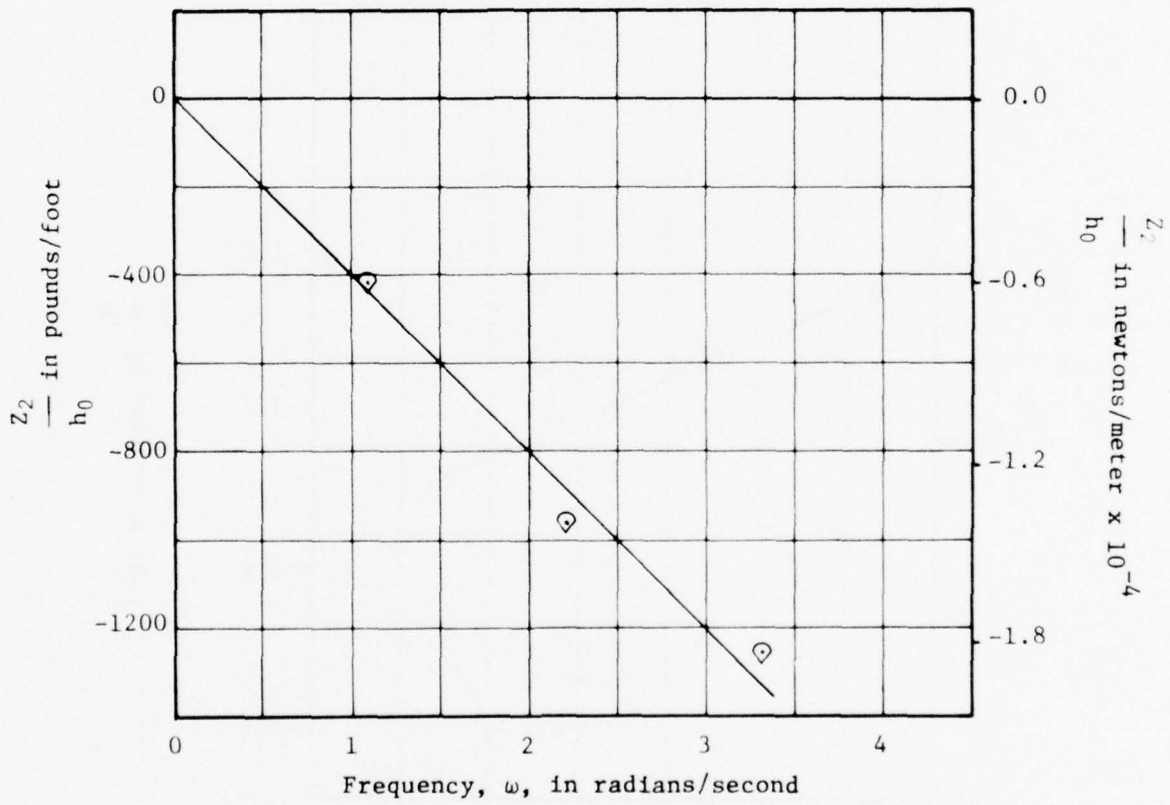
Figure 27 - Variation of Out-of-Phase Heave Force with
Frequency for a 2-3-2 Fan Configuration at
12 Knots by Heaving Technique
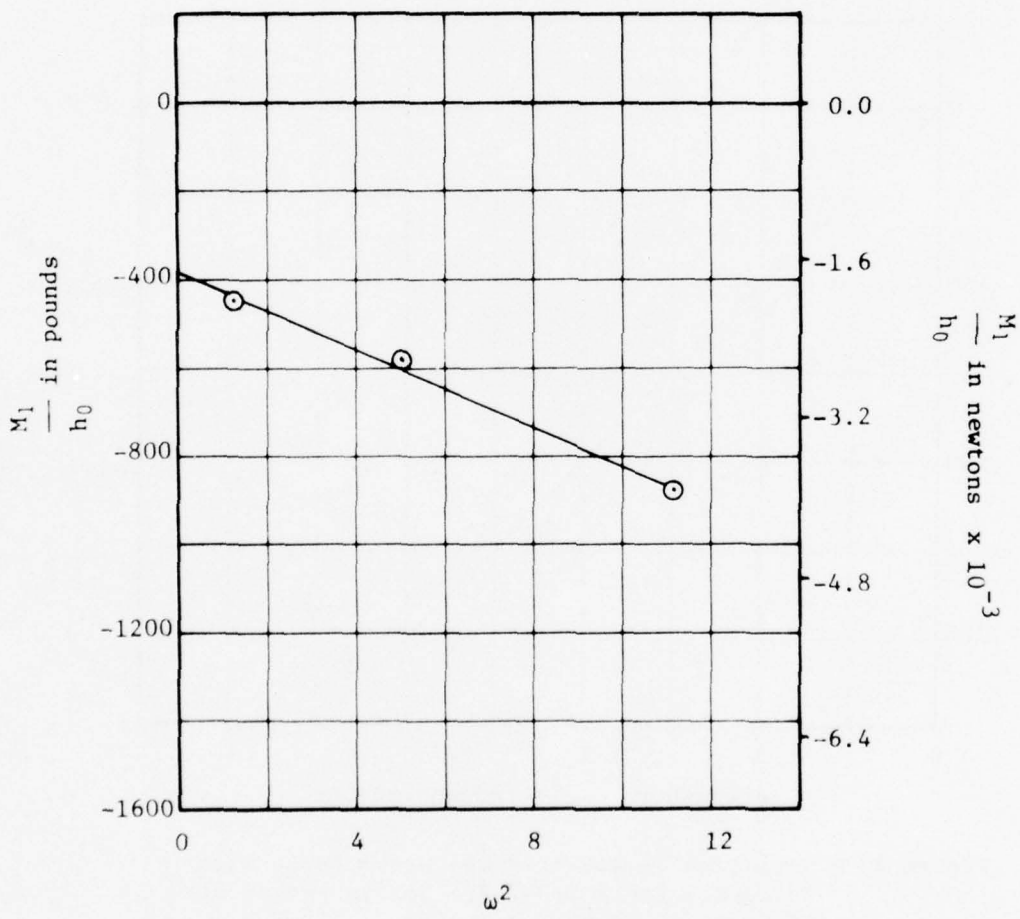
Figure 28 - Variation of In-Phase Pitch Moment with Frequency
Squared for a 2-3-2 Fan Configuration at 12 Knots
by Heaving Technique
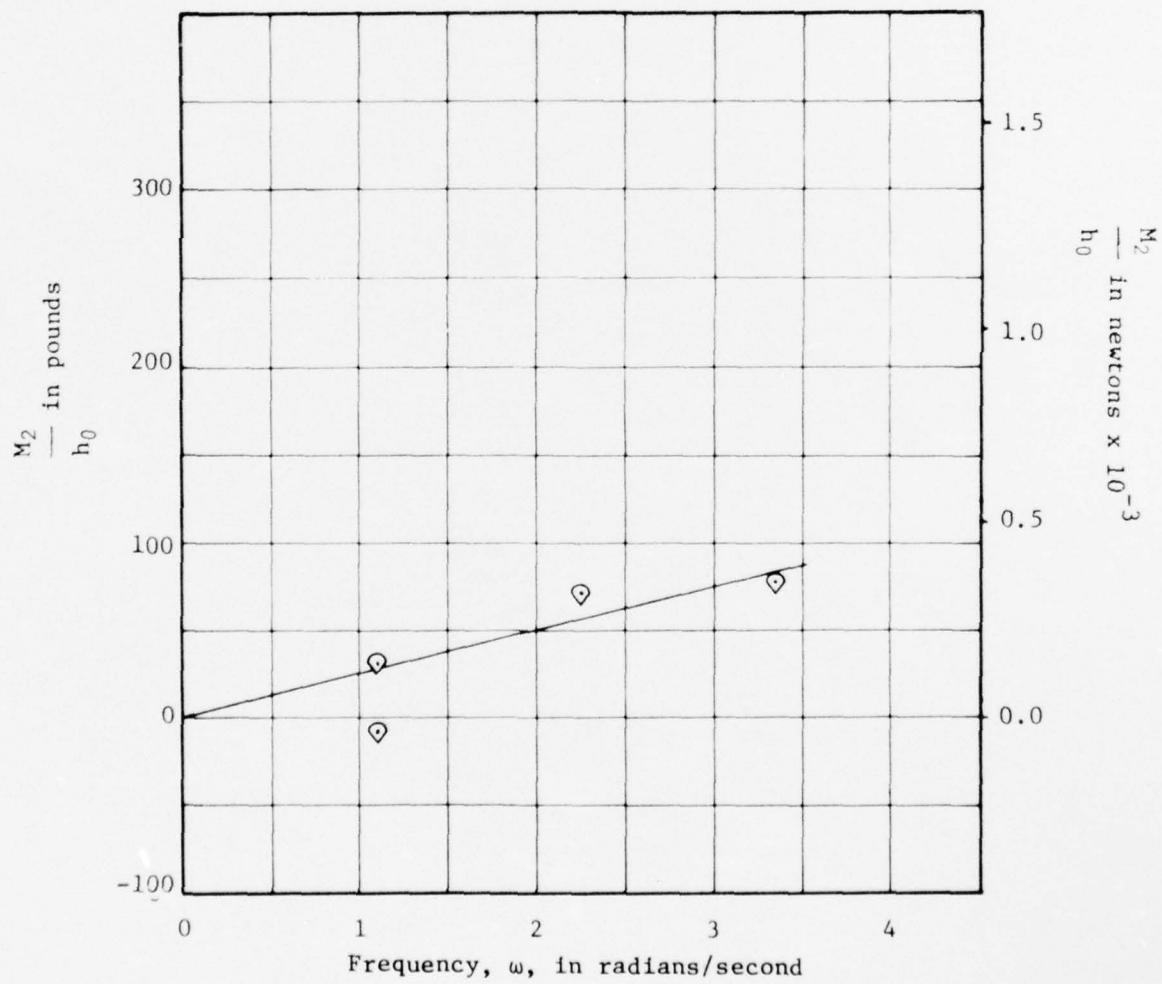
Figure 29 - Variation of Out-of-Phase Pitch Moment with
Frequency for a 2-3-2 Fan Configuration at
12 Knots by Heaving Technique

APPENDIX B

(Figures 30 thru 41)
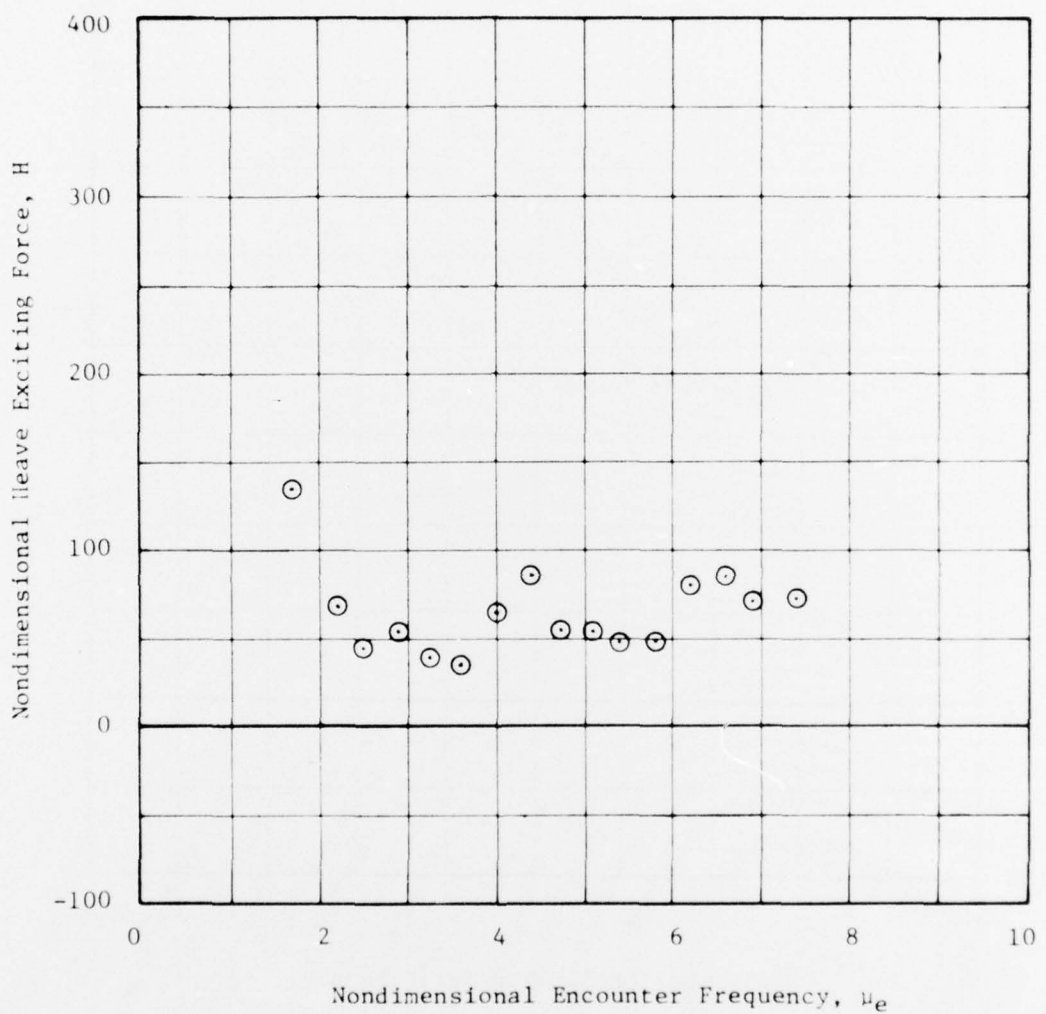
Figure 30 - Variation of Nondimensional Heave Exciting
Force with Nondimensional Encounter Frequency
at a Speed of 6 Knots by Transient Wave Technique

57
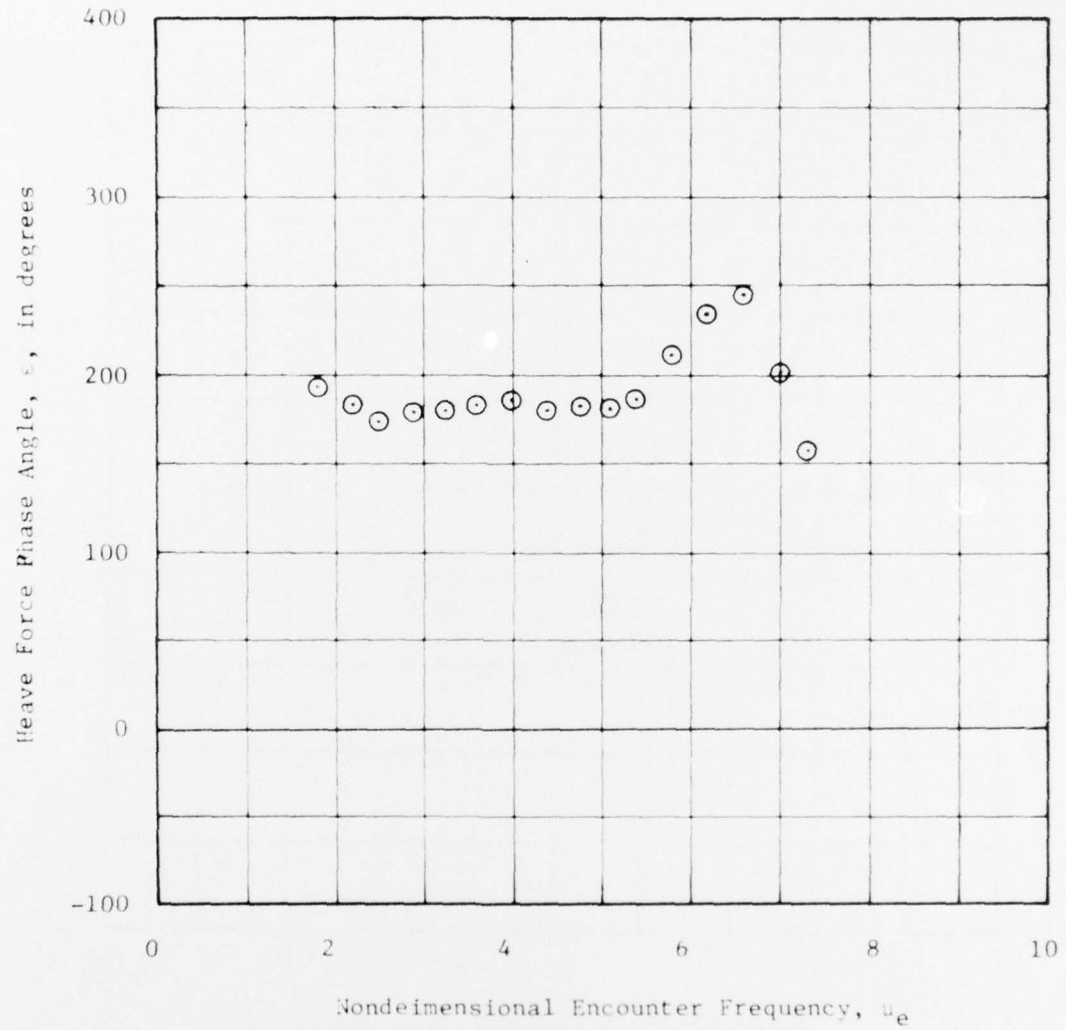
Figure 31 - Variation of Heave Exciting Force Phase Angle with
Nondimensional Encounter Frequency at a Speed of
6 Knots by Transient Wave Technique
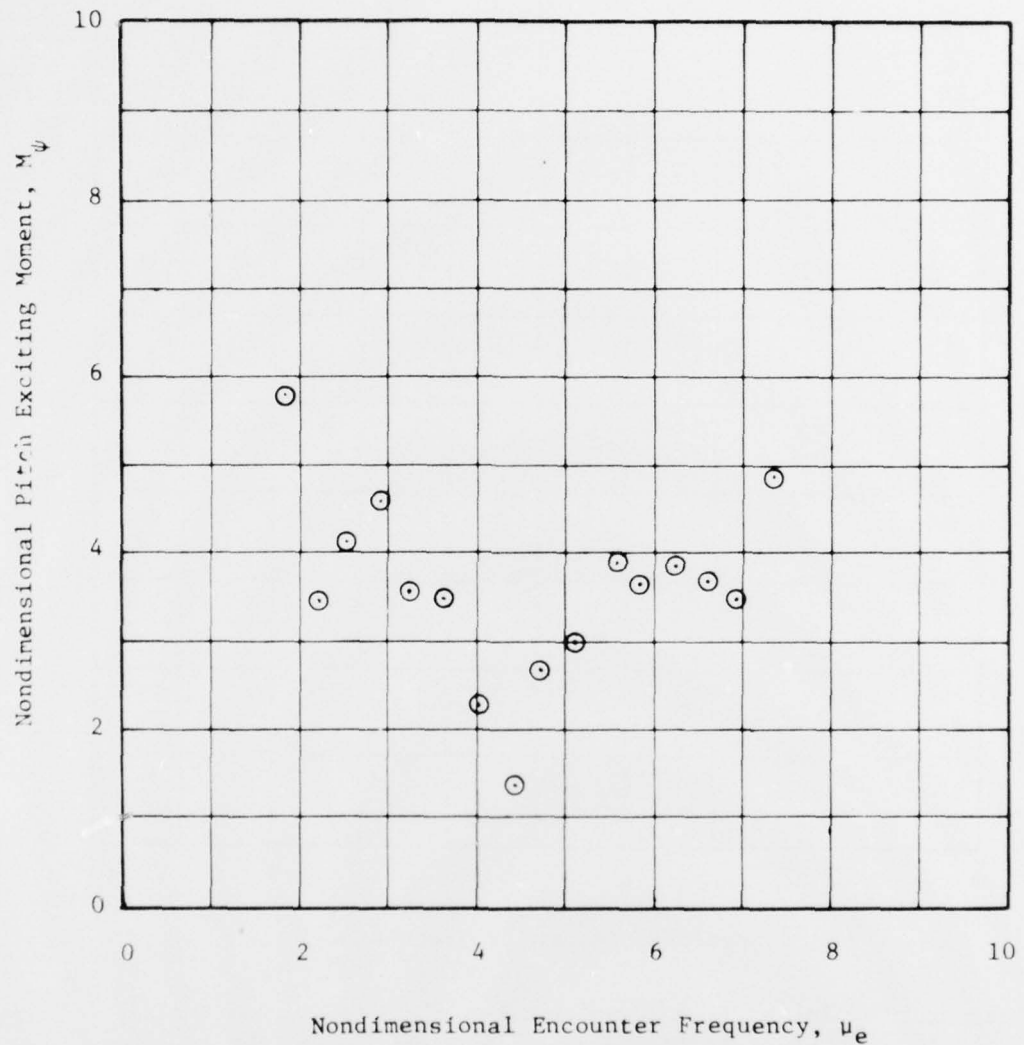
Figure 32 - Variation of Nondimensional Pitch Exciting Moment with
Nondimensional Encounter Frequency at a Speed of 6 Knots
by Transient Wave Technique
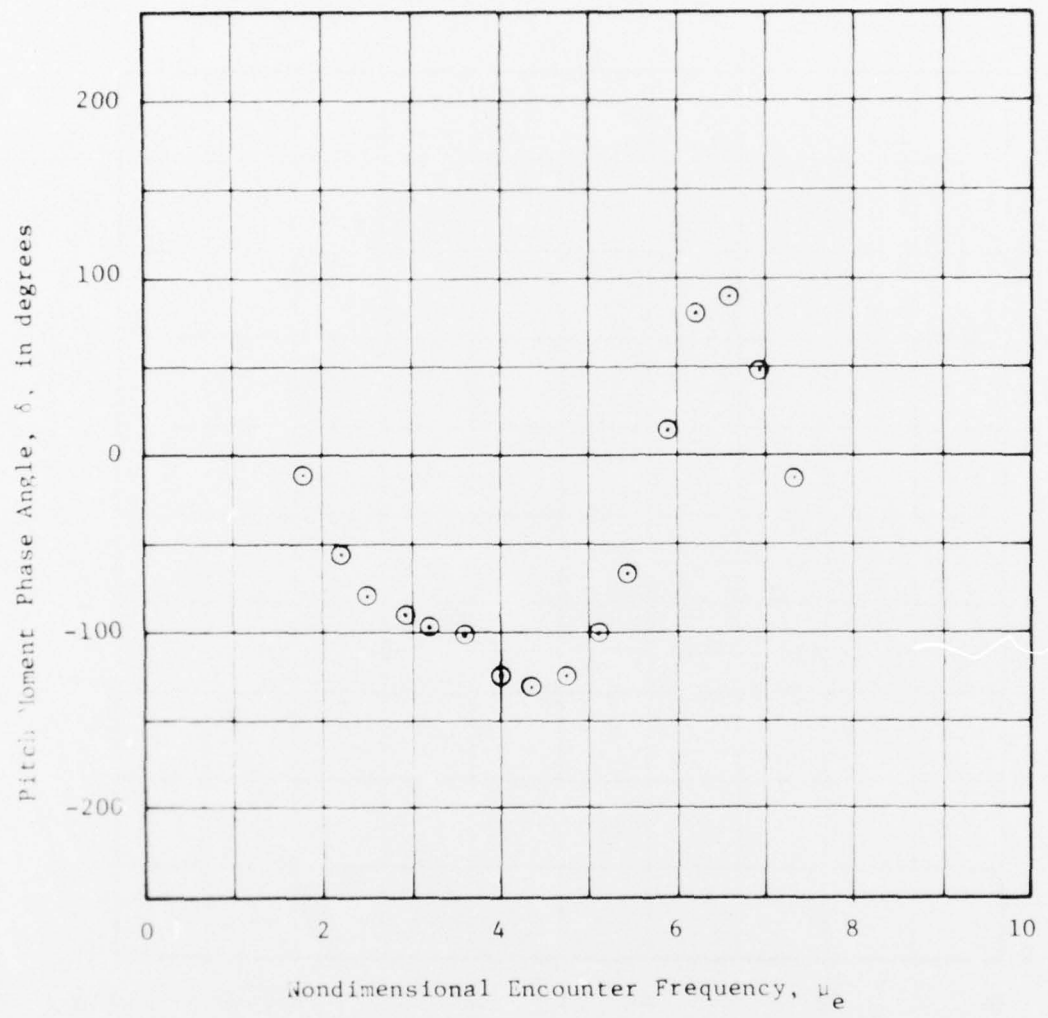
Figure 33 - Variation of Pitch Phase Angle with Nondimensional
Encounter Frequency at a Speed of 6 Knots by
Transient Wave Technique

60
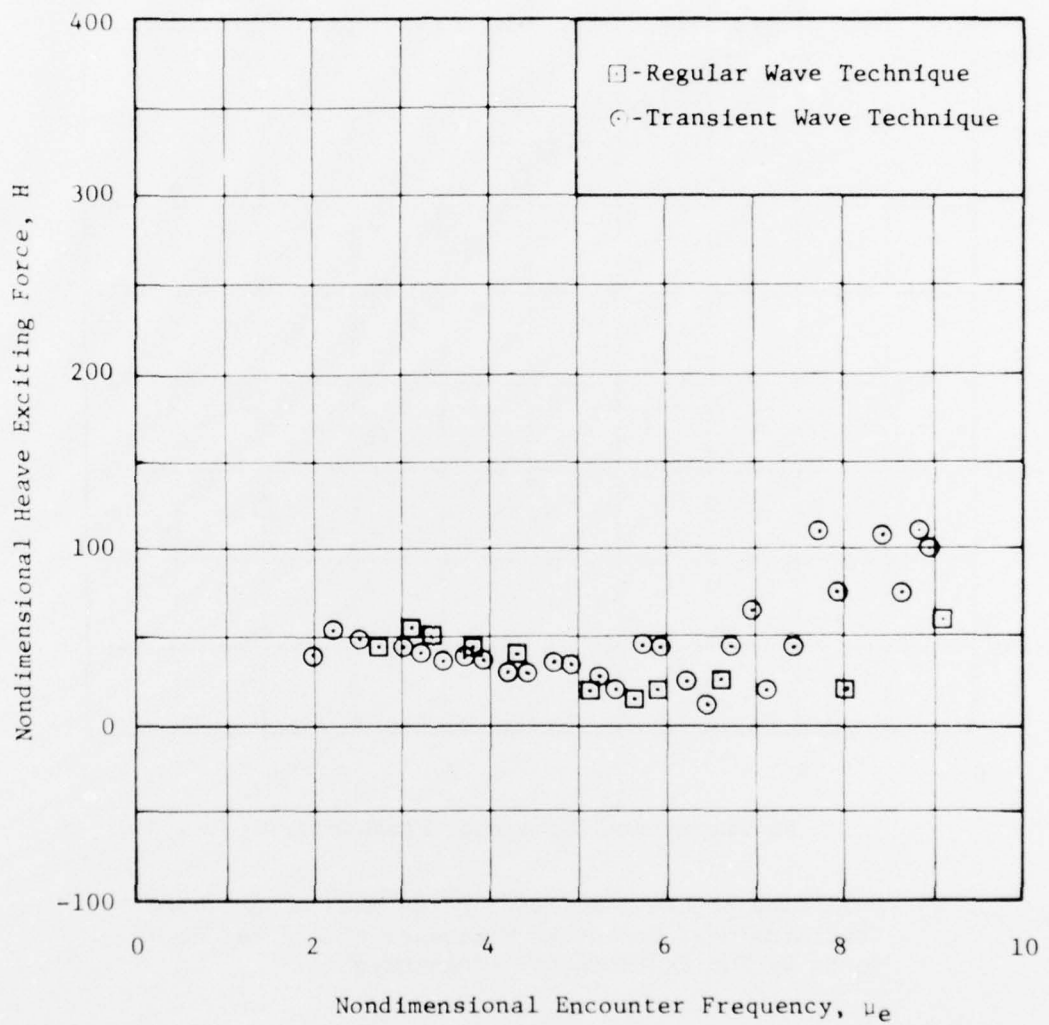
Figure 34 - Variation of Nondimensional Heave Exciting Force with Nondimensional Encounter Frequency at a Speed of 9 Knots by Two Experimental Techniques

61
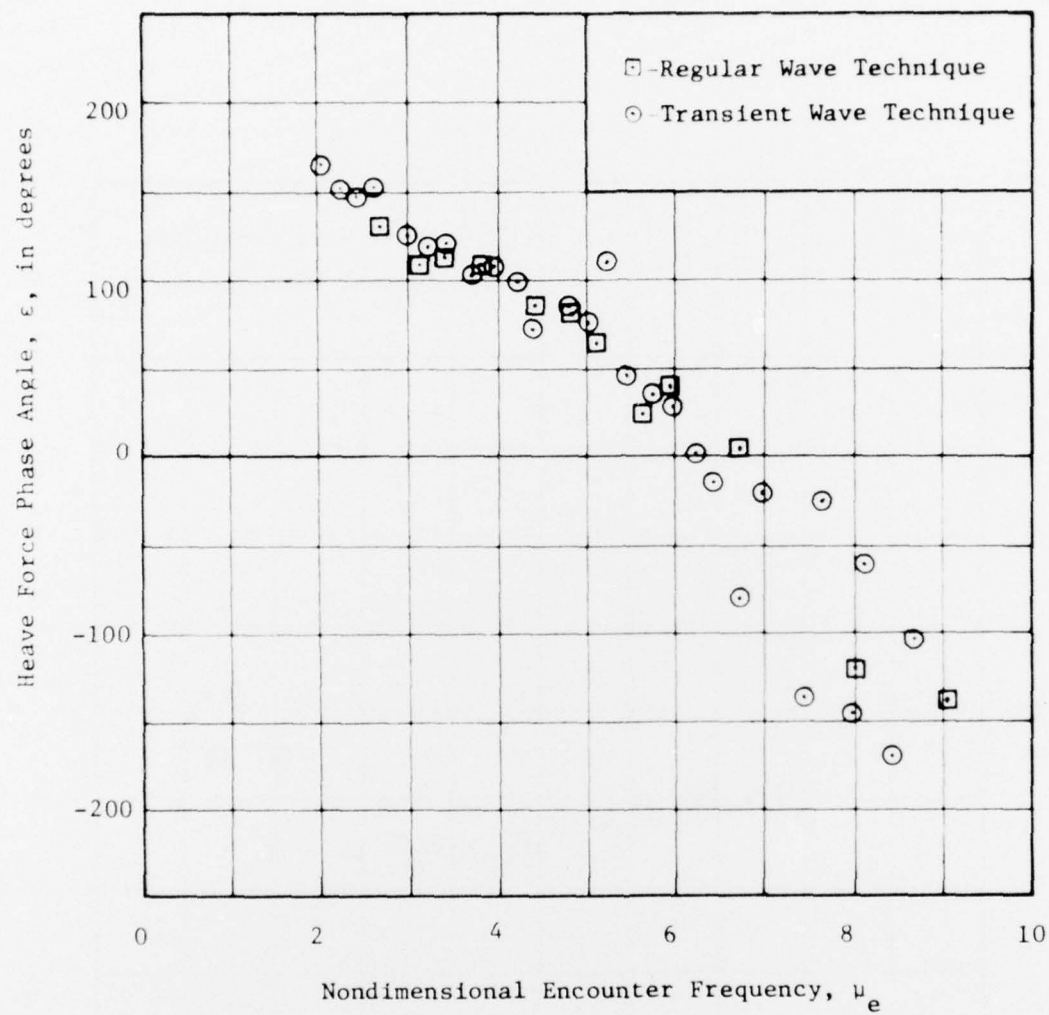
Figure 35 - Variation of Heave Exciting Force Phase Angle with
Nondimensional Encounter Frequency at a Speed of 9
Knots by Two Experimental Techniques
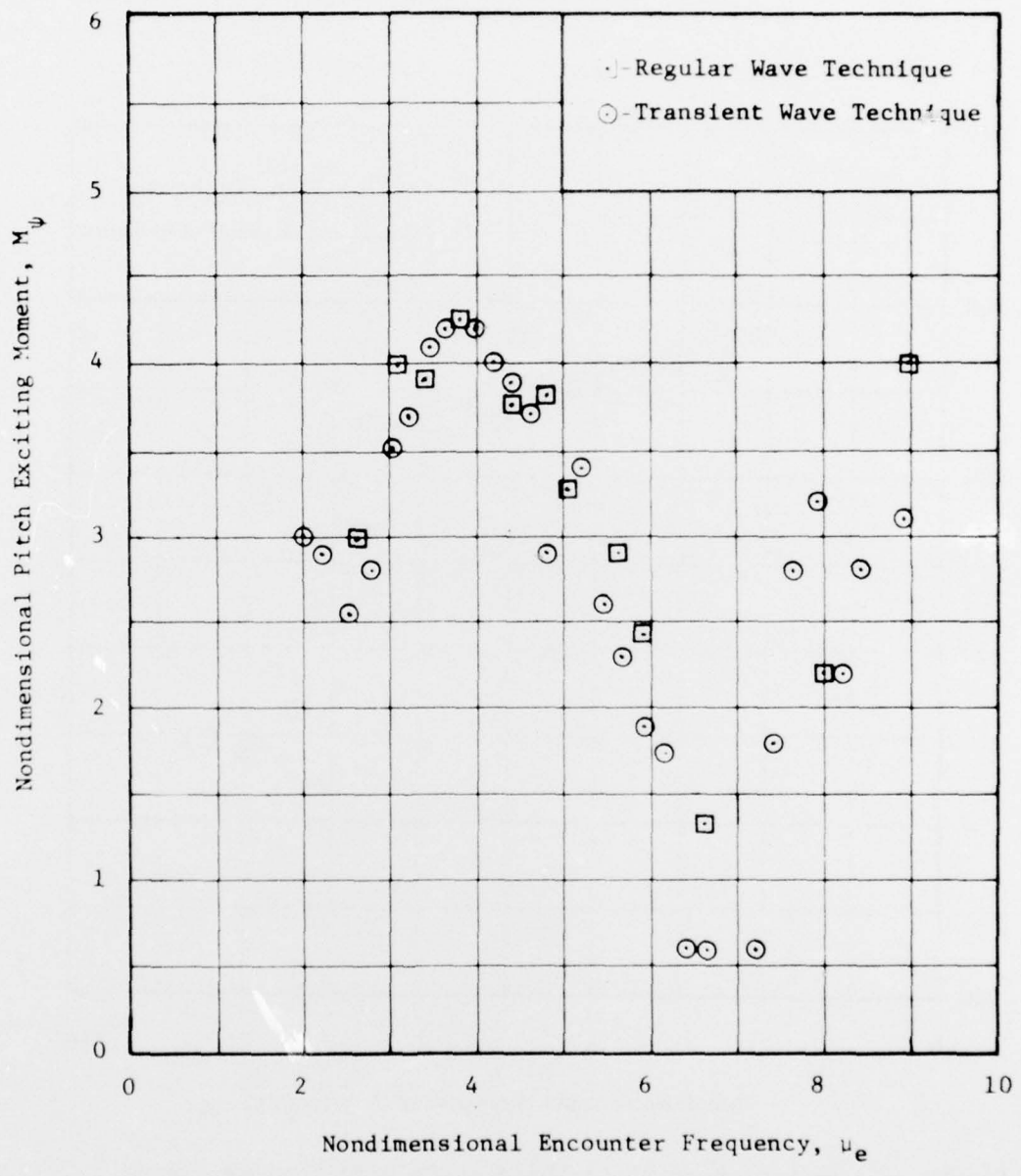
Figure 36 - Variation of Nondimensional Pitch Exciting Moment with
Nondimensional Encounter Frequency at a Speed of 9 Knots
by Two Experimental Techniques

63
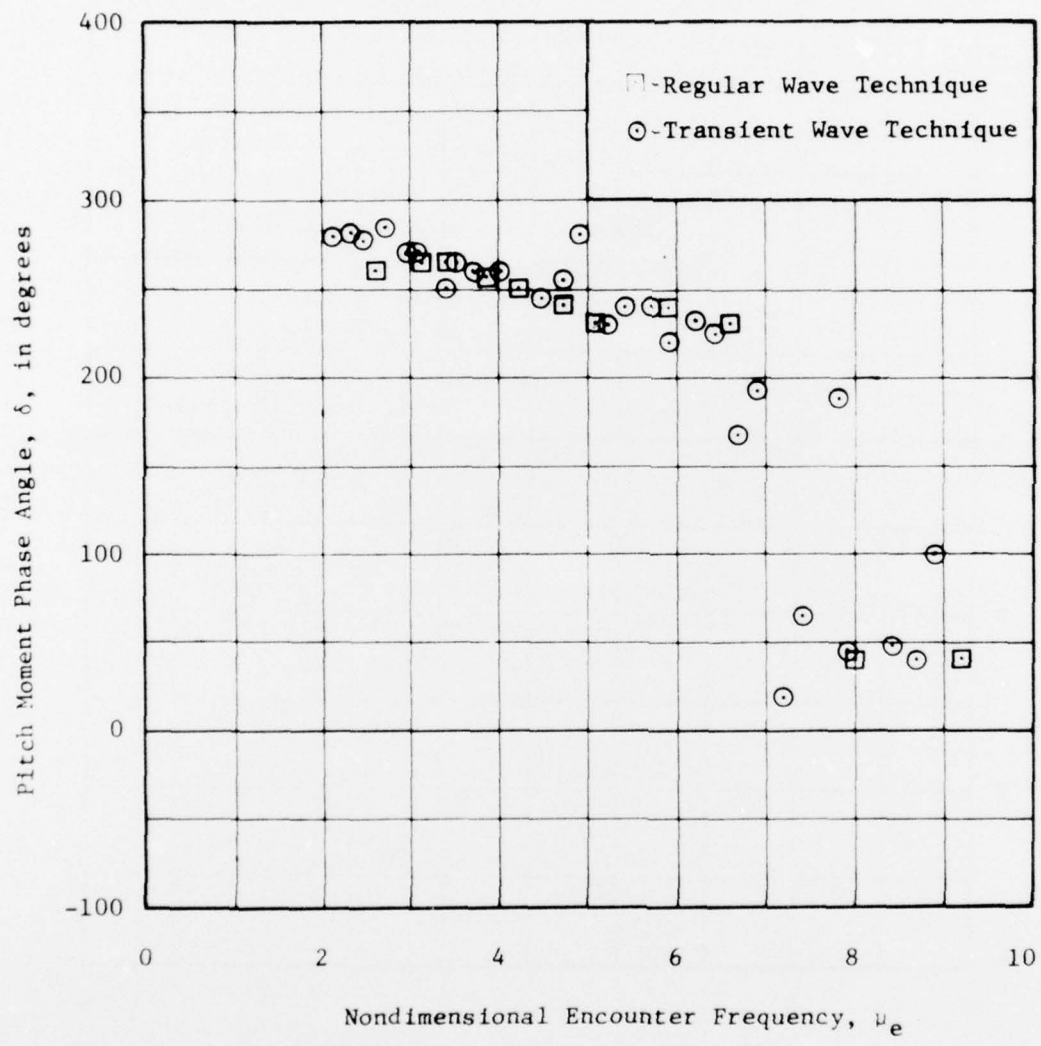
Figure 37 – Variation of Pitch Phase Angle with Nondimensional
Encounter Frequency at a Speed of 9 Knots by Two
Experimental Techniques
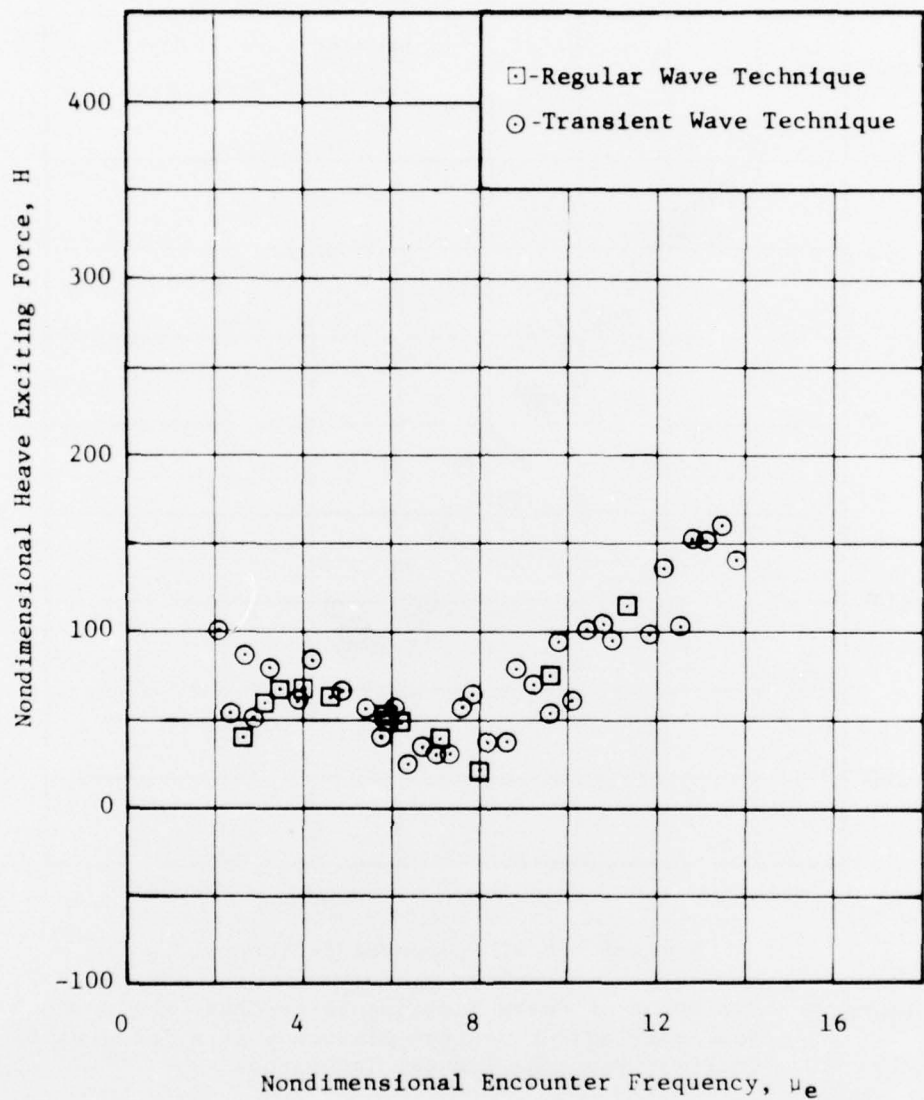
Figure 38 -Variation of Nondimensional Heave Exciting Force
with Nondimensional Encounter Frequency at a
Speed of 12 Knots by Two Experimental Techniques
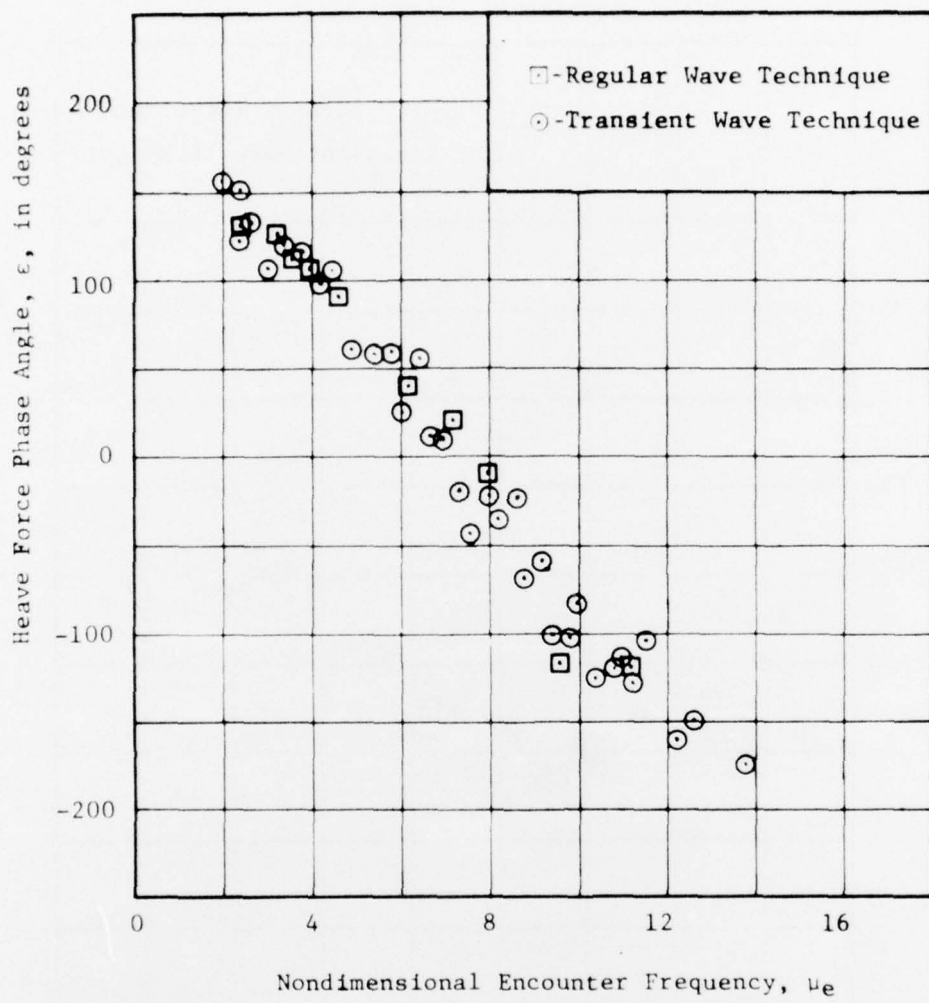
Figure 39 – Variation of Heave Exciting Force Phase Angle with
Nondimensional Encounter Frequency at a Speed of 12
Knots by Two Experimental Techniques

66
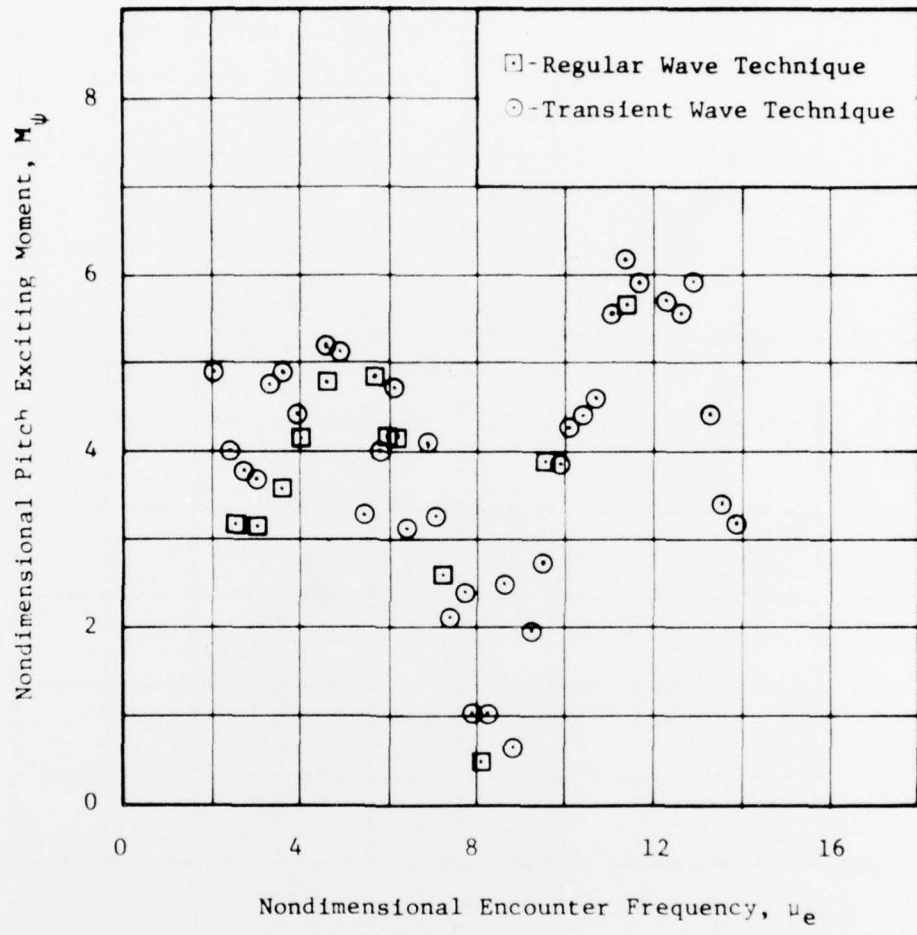
Figure 40 - Variation of Nondimensional Pitch Exciting Moment with Nondimensional Encounter Frequency at a Speed of 12 Knots by Two Experimental Techniques
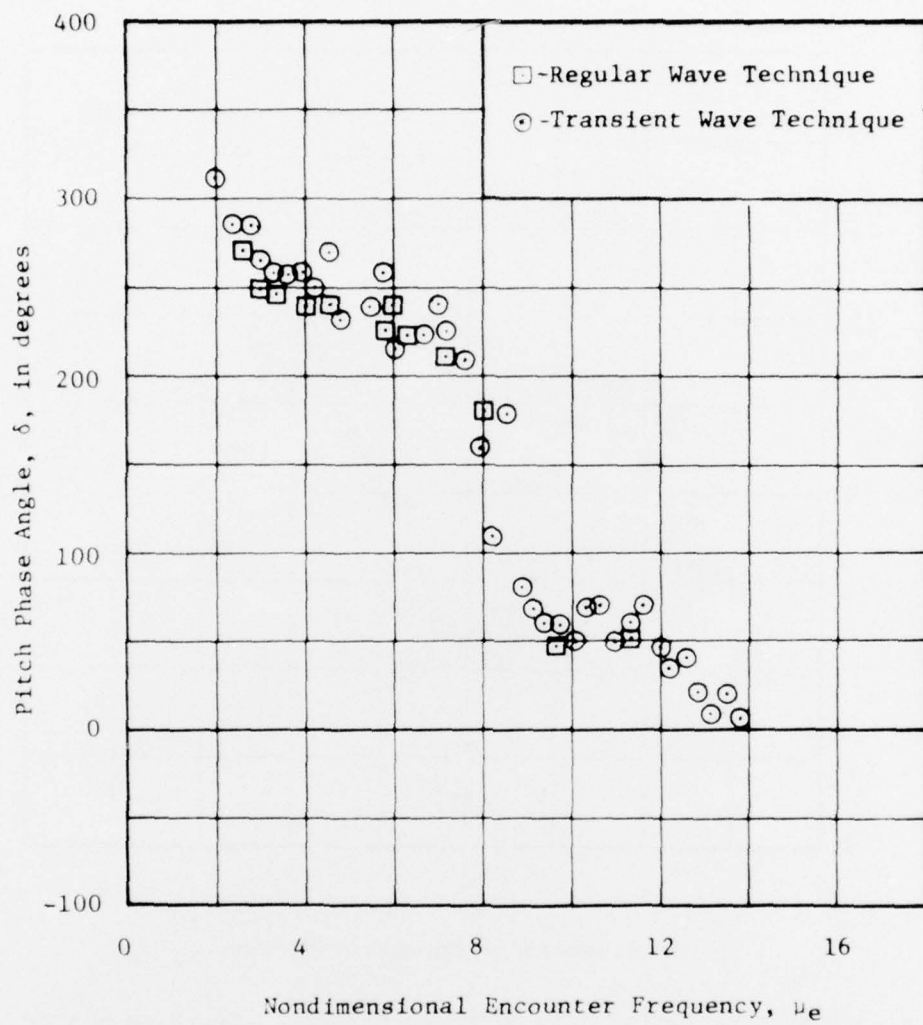
Figure 41 - Variation of Pitch Phase Angle with Nondimensional
Encounter Frequency at a Speed of 12 Knots by Two
Experimental Techniques

DTNSRDC ISSUES THREE TYPES OF REPORTS

(1) DTNSRDC REPORTS, A FORMAL SERIES PUBLISHING INFORMATION OF PERMANENT TECHNICAL VALUE, DESIGNATED BY A SERIAL REPORT NUMBER.

(2) DEPARTMENTAL REPORTS, A SEMIFORMAL SERIES, RECORDING INFORMA TION OF A PRELIMINARY OR TEMPORARY NATURE, OR OF LIMITED INTEREST OR SIGNIFICANCE, CARRYING A DEPARTMENTAL ALPHANUMERIC IDENTIFICATION.

(3) TECHNICAL MEMORANDA, AN INFORMAL SERIES, USUALLY INTERNAL WORKING PAPERS OR DIRECT REPORTS TO SPONSORS, NUMBERED AS TM SERIES REPORTS, NOT FOR GENERAL DISTRIBUTION.